Pacific Northwest
NATIONAL LABORATORY

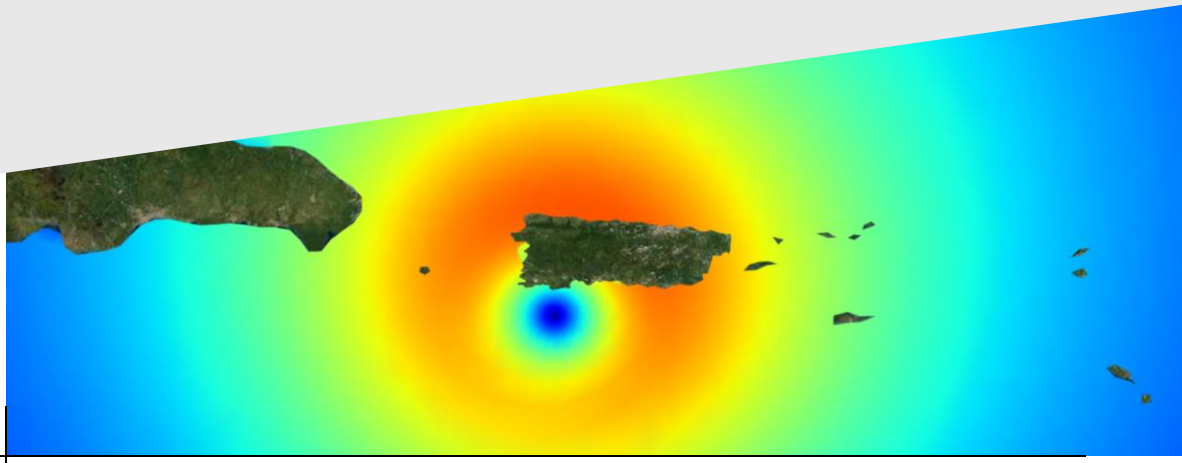

PNNL-33077

Coupled wave-current modeling for hydrodynamic load analysis of macroalgae cultivation farms

March 2023

1 Fadia Ticona Rollano
2 Zhaoqing Yang
3 Taiping Wang

U.S. DEPARTMENT OF ENERGY

Prepared for the U.S. Department of Energy
under Contract DE-AC05-76RL01830

DISCLAIMER

PACIFIC NORTHWEST NATIONAL LABORATORY
operated by
BATTELLE
for the
UNITED STATES DEPARTMENT OF ENERGY
under Contract DE-AC05-76RL01830

Printed in the United States of America

Available to DOE and DOE contractors from the
Office of Scientific and Technical Information,
P.O. Box 62, Oak Ridge, TN 37831-0062;
ph: (865) 576-8401
fax: (865) 576-5728
email: reports@adonis.osti.gov

Available to the public from the National Technical Information Service
5301 Shawnee Rd., Alexandria, VA 22312
ph: (800) 553-NTIS (6847)
email: orders@ntis.gov <https://www.ntis.gov/about>
Online ordering: http://www.ntis.gov

PNNL-33077

Coupled wave-current modeling for hydrodynamic load analysis of macroalgae cultivation farms

March 2023

1 Fadia Ticona Rollano
2 Zhaoqing Yang
3 Taiping Wang

Prepared for
the U.S. Department of Energy
under Contract DE-AC05-76RL01830

Pacific Northwest National Laboratory
Seattle, Washington 98109

Acknowledgments

This research was funded through a subcontract with the Marine Biological Laboratory, University of Chicago as part of the Tropical Seaweed Farm Project, funded by the Advanced Research Projects Agency-Energy (ARPA-E) Macroalgae Research Inspiring Novel Energy Resources (MARINER) program.

Kerry Emanuel from the Massachusetts Institute of Technology for providing a dataset of synthetic hurricane tracks in Puerto Rico. William J. Pringle, Brian R. Joyce, and Joannes J. Westerink from the University of Notre Dame for providing the unstructured grid (PRVI15) that was adapted for this study.

Acronyms and Abbreviations

ARPA-E	Advanced Research Projects Agency-Energy
AOI	area of influence
CarICOOS	Caribbean Integrated Coastal Ocean Observing System
FL	Florida
MARINER	Macroalgae Research Inspiring Novel Energy Resources
NCEP	National Centers for Environmental Prediction
NDBC	National Data Buoy Center
NOAA	National Oceanic and Atmospheric Administration
MBL	Marine Biological Laboratory
POI	point of interest
PR	Puerto Rico
SMS	Surface-water Modeling System
SWAN	Simulating WAves Nearshore

Contents

Figures

Tables

1.0 Introduction

Large-scale cultivation of macroalgae is one of the most promising biofuel sources that could reduce our consumption of fossil fuels (Langlois et al. 2012; Rhodes 2010; Notoya 2010; Menetrez 2012) and would be particularly economically competitive when grown for the co-production of additional goods such as food and textiles (Milledge et al. 2014). Current production of biofuel from algal biomass is limited by labor costs and lack of data on potential impacts of cultivation and harvesting on marine and coastal environments as well as a comprehensive characterization of the impact of environmental conditions on macroalgal feedstock and their bioproduct and biofuel yield and quality. As part of the Macroalgae Research Inspiring Novel Energy Resources (MARINER) program, funded by the United States (U.S.) Department of Energy (D.O.E.) Advanced Research Projects Agency-Energy (ARPA-E), the Marine Biological Laboratory (MBL) has been developing a test system for tropical seaweed cultivation in the Gulf of Mexico and the Caribbean.

An integral step in designing macroalgae cultivation farms is to adequately characterize the hydrodynamic climate at potential growth sites. In regions like the Gulf of Mexico and the Caribbean, which are highly exposed to tropical cyclones, it is critical to not only consider the day-to-day hydrodynamic conditions but to also assess the risk of extreme sea states to ensure the survivability of future macroalgae farms. Under these considerations, the Pacific Northwest National Laboratory (PNNL) is providing modeling support for MBL to inform the design and siting of the farm systems that have been proposed for MBL's MARINER project.

This report describes the development of a high-resolution coupled storm surge and wave model to simulate the hydrodynamics and wave climate at proposed macroalgae cultivation sites preselected by MBL in Florida and Puerto Rico. Model results, including model validation, water level, current distributions, and sea states, are discussed for both selected sites in Florida and Puerto Rico coast. These simulations provide an accurate insight into the hydrodynamic conditions that a macroalgae farm is likely to experience during its operational lifetime, including current information to support fine-scale hydrodynamic load modeling, risk analysis and system design.

2.0 Methods

2.1 Study domain

Based on a preliminary analysis, MBL identified two sites in Florida suitable for macroalgae cultivation and another three in Puerto Rico (Figure 1). The arrays in Florida, FL1 and FL2 shown in Figure 1.b, are located just outside of Tampa Bay. FL1 is situated at a 5.8 m water depth 1.2 km away from the shore while F2 is at a 7.2 m water depth and 3.3 km away from the shore. In Puerto Rico the three proposed arrays are situated in La Parguera on the shoreside of cays and coral reefs: Cayo Enrique, Cayo Media Luna, and Arrecife Romero. The Cayo Enrique array is situated at a 17 m water depth 2 km from the shore and is the most sheltered. The Cayo Media Luna array is in 17.5 m of water at 3.4 km from the shore and is the least sheltered. The Arrecife Romero array is at a 11.7 depth and is 3 km away from the coast; it is located just shoreward from the opening between two reef features.

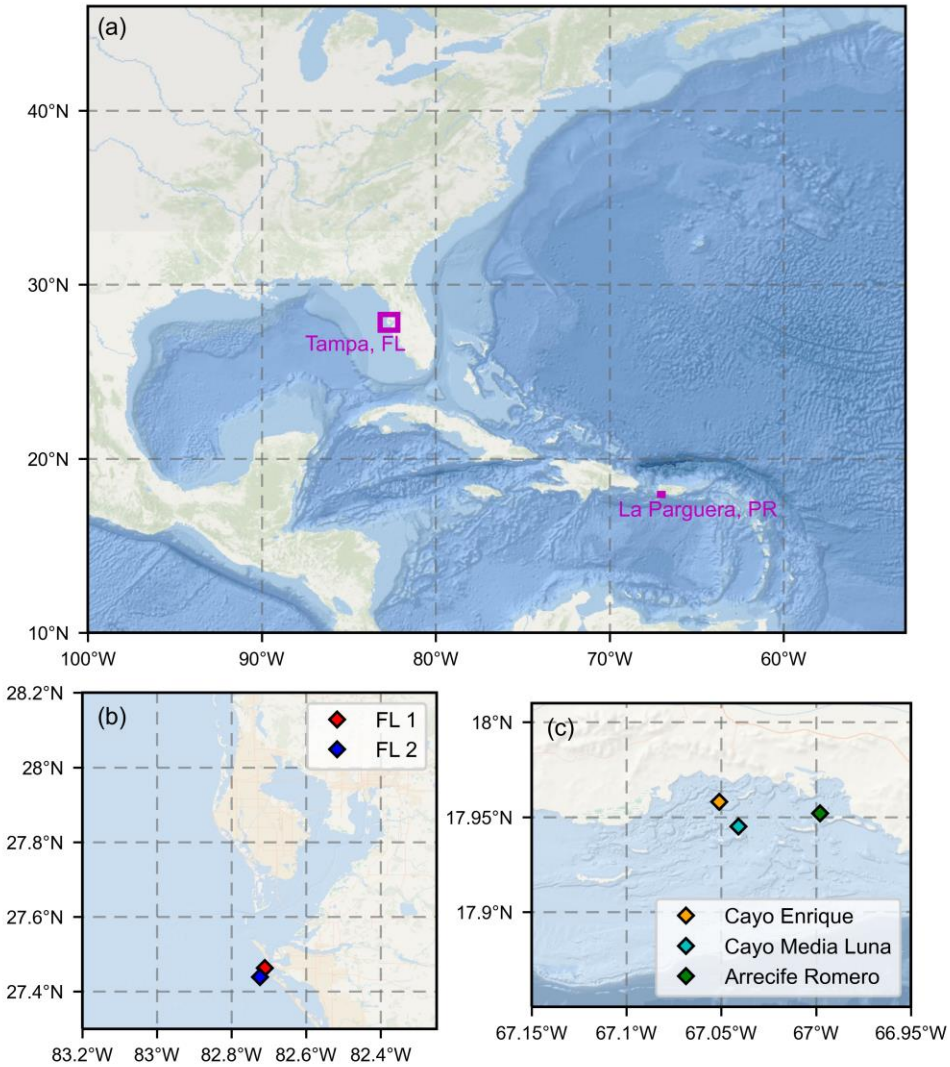

Figure 1. (a) Study domain showing general location of study sites. Location maps of potential macroalgae arrays in (b) Tampa, Florida and (c) La Parguera, Puerto Rico.

2.2 Model description

The numerical models selected for this project are ADCIRC v53.04, an ocean circulation model, and Simulating WAves Nearshore (SWAN) v41.10, a third-generation spectral wave model. These models have been previously integrated into a coupled system for storm surge studies of historical hurricanes (Dietrich, Zijlema, et al. 2011; Dietrich, Westerink, et al. 2011) and recently on a study of the influence of buoyant submerged aquatic vegetation, such as seagrasses and kelps, on estuarine hydrodynamics (Holzenthal, Hill, and Wengrove 2022).

For this project, the coupled ADCIRC+SWAN system, executed in a three-dimensional (3D) mode and paired with an unstructured grid, was used to simulate the hydrodynamic climate in Florida and Puerto Rico under normal operation conditions (described in more detail in Section 2.4.1) and in Puerto Rico under storm conditions (described in Section 2.4.2).

An unstructured mesh was developed based on the PRVI15 grid presented in (Joyce et al. 2019) with modifications around Puerto Rico and Florida coast. The model domain encompasses the U.S. east coast, the Gulf of Mexico, and the Caribbean with an open boundary in the North Atlantic Ocean to resolve any significant offshore influences by tropical cyclones. The shoreline and bathymetry generally follow that of the PRVI15 grid (Figure 2).

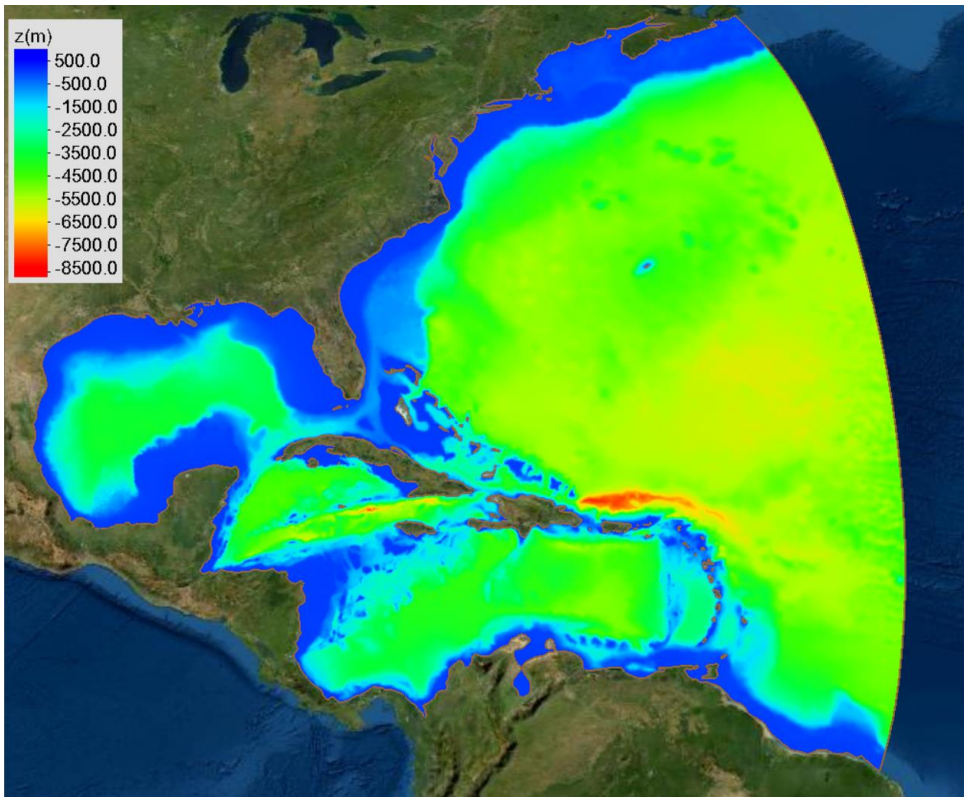

Figure 2. Model domain and bathymetry.

Using Surface-water Modeling System (SMS), the PRVI15 grid was adapted to include fine spatial resolution near the proposed macroalgae cultivation sites, and lower, depth-dependent, resolution elsewhere. Figure 3 shows the element size of the model mesh. The mesh is composed of 194,000 triangular elements and, except at areas of interest, it has a 10 km coastal resolution relaxed to 65 km in deep water. Figure 4 shows the regions that have

increased model resolution in Tampa, Florida and La Parguera, Puerto Rico. At these locations, the average size of the grid elements is about 100 m along the coastline relaxed smoothly to about 3 km offshore.

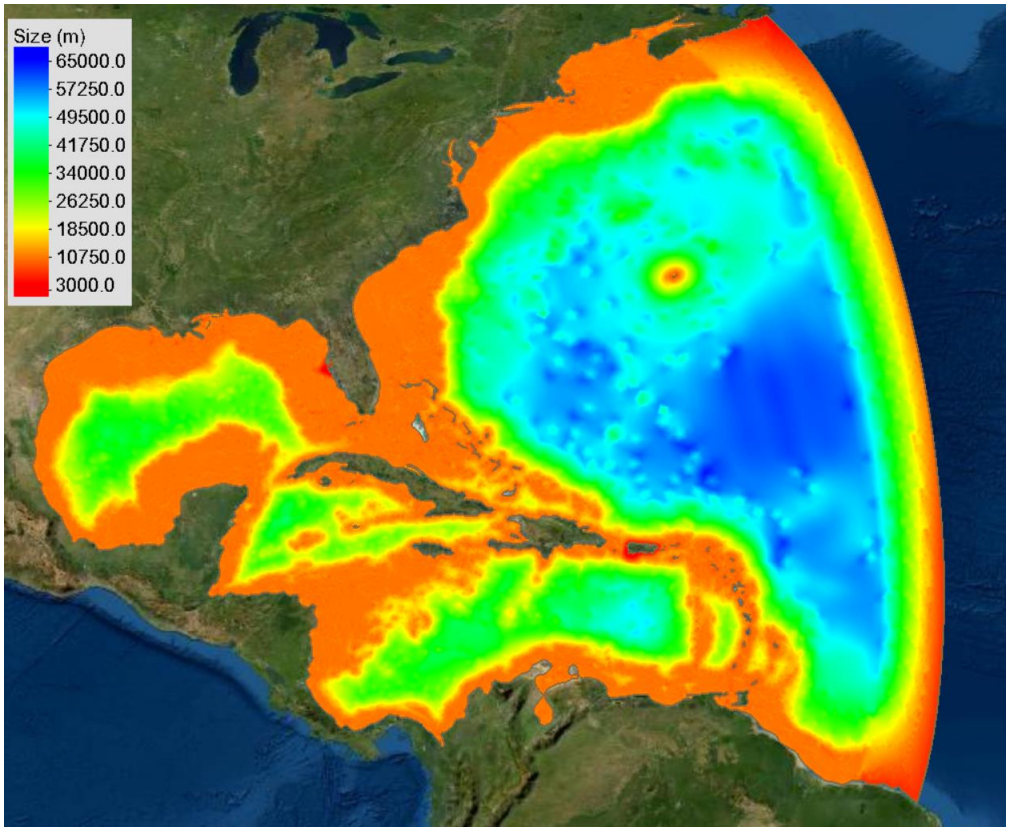

Figure 3. Size of unstructured mesh triangular elements.

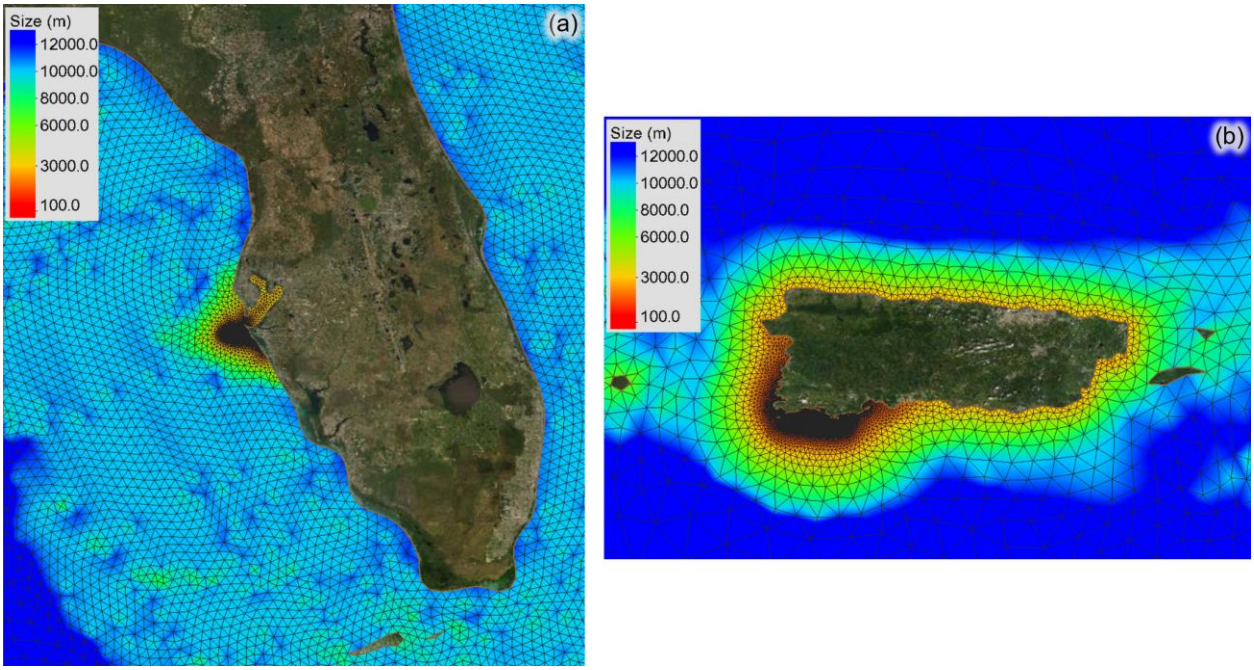

Figure 4. Regions of greatest grid resolution (a) Tampa, FL and (b) La Parguera, PR.

2.3 Data for model validation and boundary forcing

Two distinct sets of simulations were executed to (1) characterize the “normal” operation conditions that the cultivation sites in Florida and Puerto Rico are most likely to experience on a day-to-day basis, and (2) to characterize the increased hydrodynamic loading that the farms in Puerto Rico would experience under hurricane conditions. The hurricane simulations in Puerto Rico are based on a dataset of synthetic hurricane tracks of varied intensities described in more detail in Section 2.4.2.

Model validation for both normal conditions and hurricane modeling is performed by comparing simulation results against measured water levels, wave heights and wave periods obtained from the National Oceanic and Atmospheric Administration (NOAA) National Data Buoy Center (NDBC). Figure 5 shows the location of the water level gauges and wave buoys used for this purpose. Error statistics for these parameters are obtained by computing commonly used metrics including root-mean square-error (RMSE), mean percentage error (PE), scatter index (SI), bias (b), and the linear correlation coefficient (R):

$$RMSE = \sqrt{\frac{\sum_{i=1}^{N}(P_i - M_i)^2}{N}}$$

$$PE = \frac{100}{N}\sum_{i=1}^{N}\frac{P_i - M_i}{M_i}$$

$$SI = \frac{RMSE}{\bar{M}}$$

$$bias = \frac{1}{N}\sum_{i=1}^{N} P_i - M_i$$

$$R = \frac{\sum_{i=1}^{N}(P_i - \bar{P})(M_i - \bar{M})}{\sqrt{\left[\sum_{i=1}^{N}(P_i - \bar{P})^2\right]\left[\sum_{i=1}^{N}(M_i - \bar{M})^2\right]}}$$

where N is the record length, M_i is the measured data and P_i is the modeled data, with bar accents representing time averages.

Also shown in Figure 5 are 2 data points (Met 1 and Met 2) corresponding to grid nodes from the Climate Forecast System Version 2 (CFSv2) produced by NOAA's National Centers for Environmental Prediction (NCEP). CFSv2 6-hourly time series of 10 m winds (Saha et al. 2011a) were retrieved at these two locations to select the normal conditions simulation periods via a wind rose analysis described in Section 2.4.1.

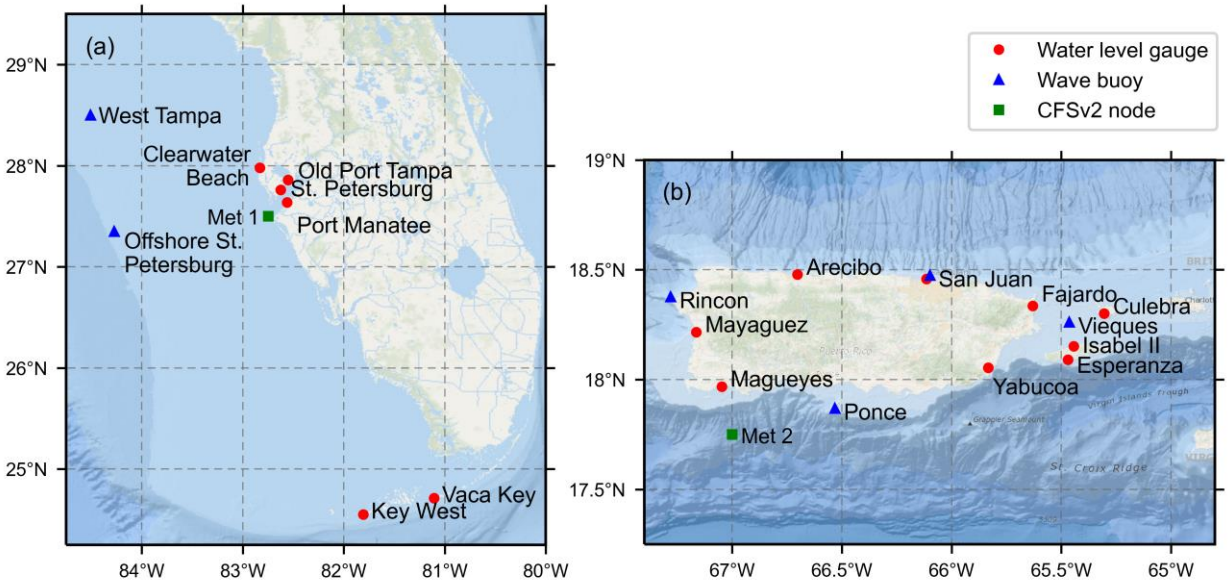

Figure 5. NDBC buoy stations and CFSv2 nodes in (a) Florida and (b) Puerto Rico.

Hourly wind and atmospheric pressure fields were retrieved from the CFSv2 database (Saha et al. 2011b) as forcing for normal condition runs and hurricane validation runs. For synthetic hurricane simulations, wind fields and atmospheric pressure fields were generated following Emanuel and Rotunno (2011) and Holland (2008) based on standard parameters corresponding to each track, including hurricane eye coordinates, maximum circular wind speed, radius of maximum circular wind and central surface pressure.

For every run, tidal forcing was provided at each node along the open boundary for the following tidal constituents: M2, O2, S2, N2, K2, K1, Q1, P1. All tidal attributes were obtained from the LeProvost dataset, available via the ADCIRC module in SMS.

2.4 Design of simulation periods

2.4.1 Normal Conditions

A wind rose analysis was performed to select periods of time that would be representative of the day-to-day operation conditions that a macroalgae farm will likely experience throughout any given year. CFSv2 6-hour wind speed records were retrieved for the last 10 full years of available data (2011-2020) at the 2 data points nearest to the proposed sites in Florida and Puerto Rico (Met 1 and Met 2 in Figure 5). At each site, wind roses were generated for each individual year, as well as for the full 10-year period, to identify a year that was most representative of the long-term conditions (Figure 6 and Figure 7).

We noticed that not much variation was present from year-to-year at La Parguera, PR, unlike in Tampa, FL, for which we continued with the wind rose analysis focused on the Met 1 station in Florida only. Comparing the Florida annual wind roses in panels (a-j) in Figure 6 with the 10-year rose in panel (k), we determined that the year 2012 was the most representative of the 10-year wind conditions because it matched the directional spread and intensity of the winds most closely. We then generated wind roses for every month in 2012 (Figure 8) to assess the annual fluctuations in wind intensity and direction at the site. We picked three months representative of the annual variability: January, May, and November. January was selected as a good representation of winter months and early spring having strong winds that can go above 7 m/s coming from the north with some western and eastern spread and from the south. May was chosen as a representative month of warmer weather with easterly and westerly winds of low to medium intensity relative to the site. November was picked to represent the conditions of September through November, having a more focused direction spread of strong northeasterly winds.

Normal condition simulations were executed with a 1-second ADCIRC time resolution and a 2-minute SWAN time resolution, exchanging data between the models every 2 minutes. Model solutions are computed at 11 uniformly distributed depths through the entire water column.

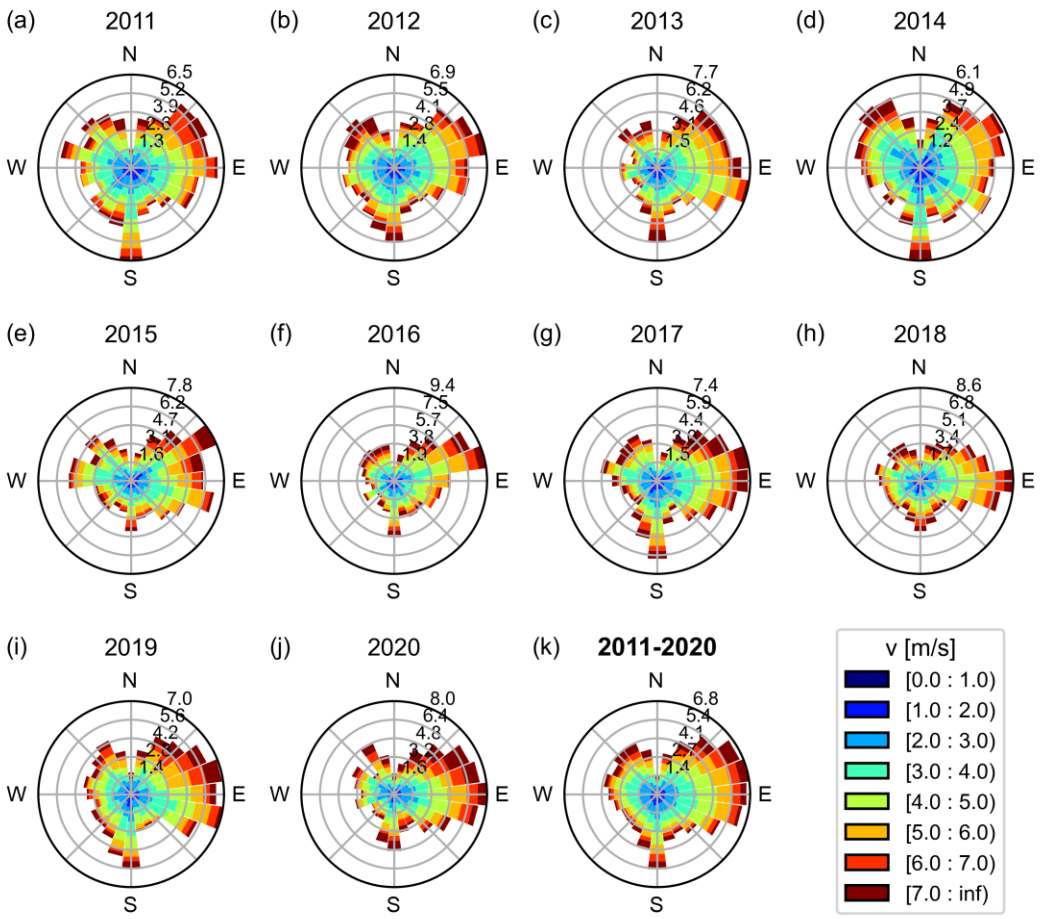

Figure 6. (a-j) Annual wind roses of CFSv2 6-hr wind speeds, and (k) wind rose of full 10-year data record, at Met 1 node in Tampa, FL.

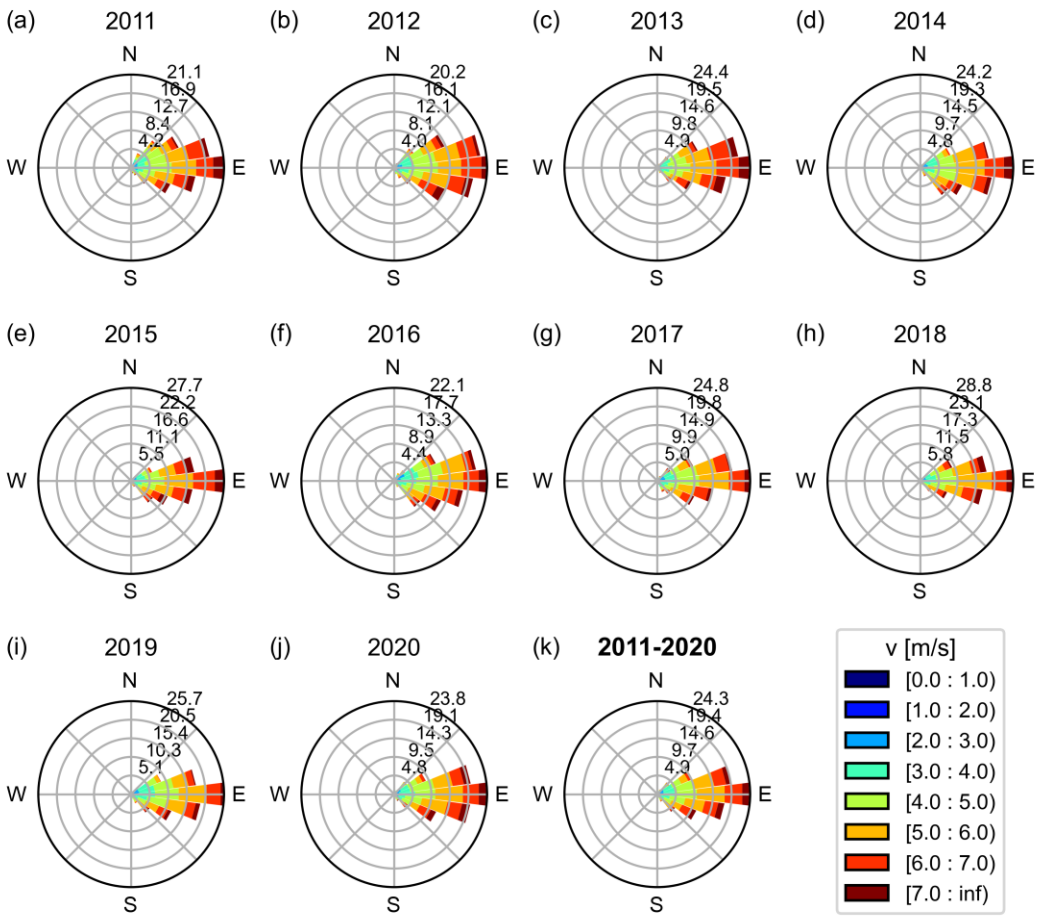

Figure 7. (a-j) Annual wind roses of CFSv2 6-hr wind speeds, and (k) wind rose of full 10-year data record, at Met 2 node in La Parguera, PR.

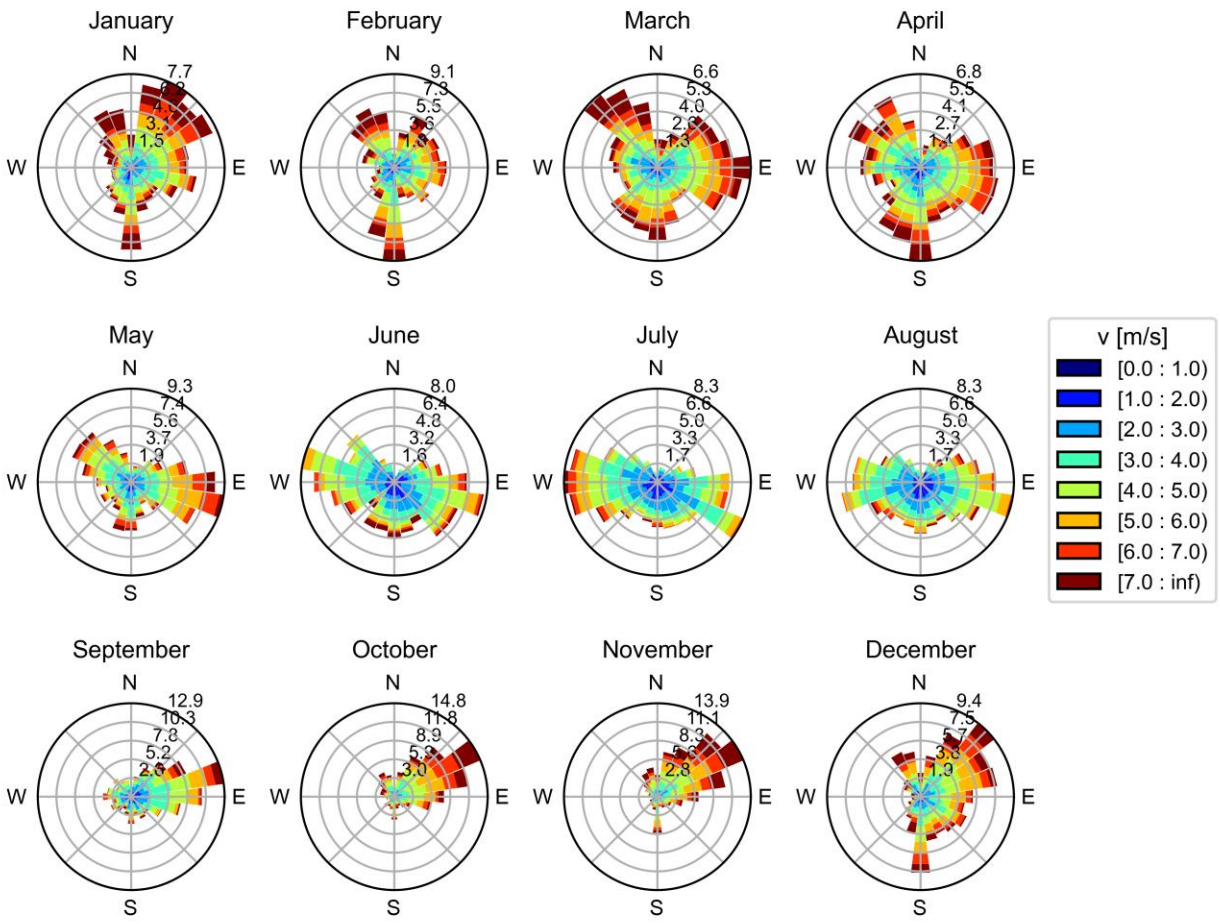

Figure 8. Monthly wind roses based on 2012 CFSv2 6-hr wind speeds at Met 1 node in Florida.

2.4.2 Synthetic hurricanes

To characterize the impacts of hurricane driven waves and currents on macroalgae farms, we solicited a dataset of synthetic storm events from Dr. Kerry Emanuel, a meteorologist from the Massachusetts Institute of Technology (MIT). The dataset contains 3,900 synthetic tropical storm and hurricane tracks that traverse across the main island of Puerto Rico or near its coast at some point of their trajectory. The tracks were generated based on actual meteorological data from 1979 to 2017 following the methods described in Emanuel et al. (2006) and are therefore representative of realistic storm events including an appropriate return period for varied storm intensities (i.e., the dataset contains a large number of lower intensity events and much fewer Category 5 events). Each track is defined in 2-hour intervals by key storm parameters, including maximum wind speed, v_m, radius of maximum wind, RMW, and central pressure, p_{cs}.

To manage the use of computer power and to focus the simulations on the cultivation sites we subsampled the original dataset through a series of filters. First, we defined a circular area of influence (AOI) 20 km in diameter and centered about a point of interest (POI) equal to the average coordinates of the 3 arrays in La Parguera, retaining only the 479 tracks crossing the AOI (Figure 9). The 479-track subset was then categorized based on the maximum wind speed of each event at the POI following the Saffir-Simpson hurricane wind scale (Table 1). The intensity of 330 events did not reach the minimum criteria to qualify as any type of hurricane

either because their overall intensity was only that of tropical storms or because they intensified elsewhere in their trajectory. Figure 10 shows the remaining 149 synthetic hurricane tracks which are used as the basis for the meteorological forcing in our ensemble hurricane simulations. This ensemble subset is well representative of hurricane events that might impact the study site in Puerto Rico over time.

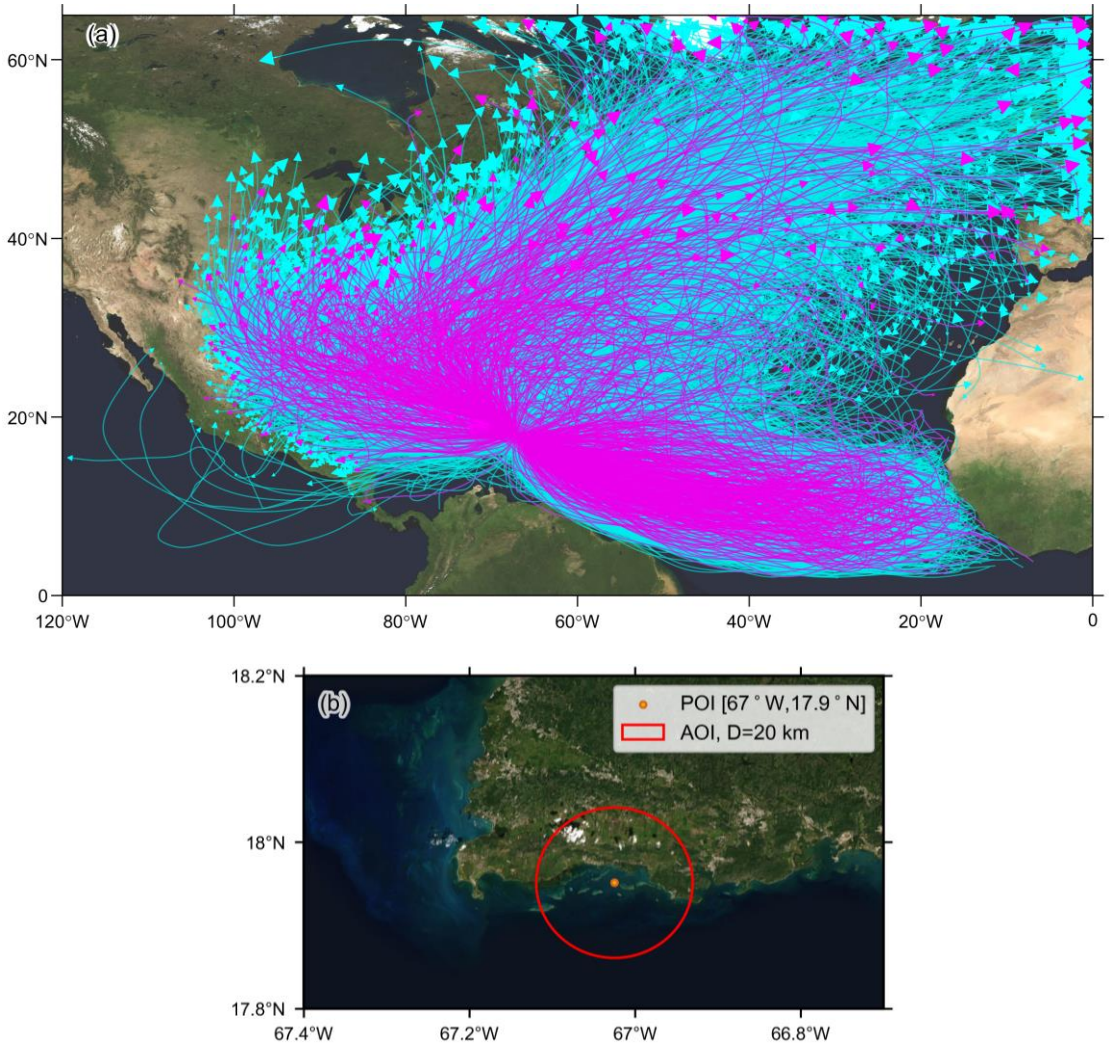

Figure 9. (a) Complete 3,900 synthetic track dataset with 479 subsampled tracks highlighted in magenta and (b) circular area of influence used to subsample the dataset.

Table 1. Breakdown of synthetic hurricane intensities

Hurricane category (Saffir-Simpson scale)	Number of tracks meeting criteria[(a)]
5 (≥70 m/s)	3
4 (58-70 m/s)	4
3 (50-58 m/s)	16
2 (43-49 m/s)	25

	1 (33-42 m/s)	101
	TOTAL	149[b]

(a) *Based on lifetime maximum wind speed at POI*

(b) *330 events do not reach hurricane intensities when passing through the POI*

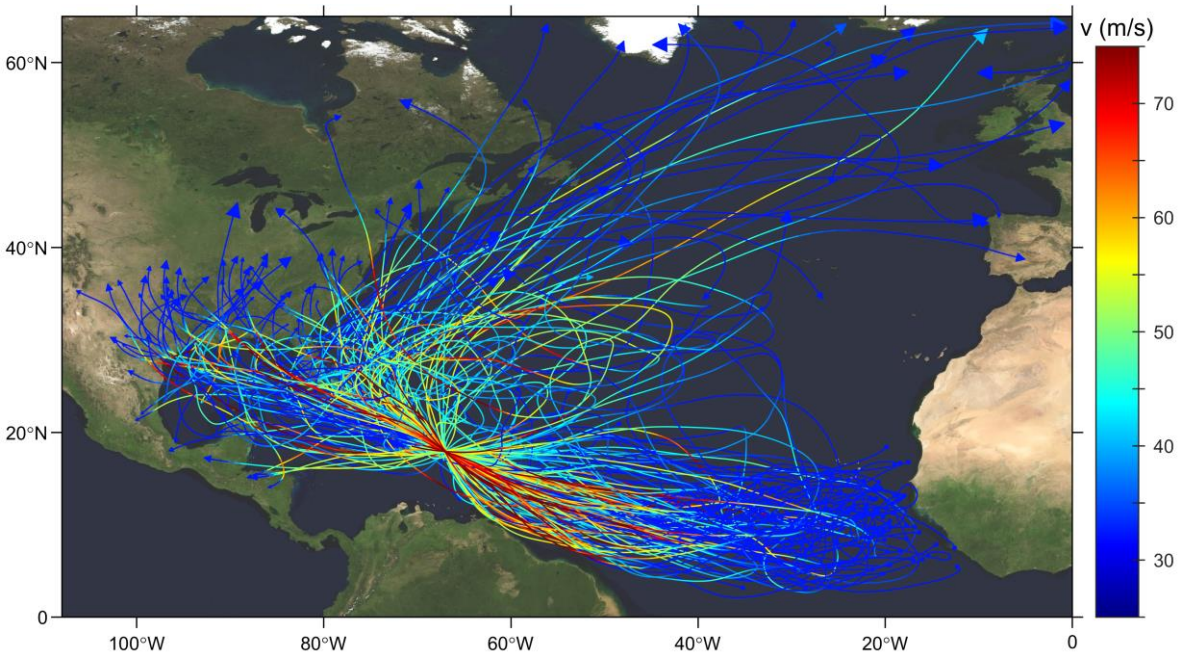

Figure 10. Synthetic hurricane tracks to be simulated colored by wind speed

Wind fields were generated following the methodology outlined in Emanuel and Rotunno (2011) from each track's time series of maximum wind speed and radius of maximum wind, and a maximum distance of storm influence set at 300 km. Pressure fields were generated following the methodology presented in Holland (2008) from time series of central pressure, accounting for pressure gradients near the maximum winds. All tracks were shortened for an event simulation duration of 5 days centered about the time of greatest storm intensity at the POI.

Hurricane simulations are executed with a 0.5-second ADCIRC time resolution and a 2-minute SWAN time resolution, exchanging data between the models every 2 minutes. Model solutions are computed at 10 uniformly distributed depths.

3.0 Model Results

3.1 Model validation for normal conditions

Results of the normal condition simulations, computed using the coupled ADCIRC+SWAN 3D model, are validated here against measured data obtained from NOAA's NDBC and CarICOOS (buoy locations are shown in Figure 5). Figure 11—Figure 16 show time records of measured and computed water surface elevation, significant wave heights, and peak wave periods at Florida NDBC buoy stations for the months of January, May, and November. Similar parameters are shown in Figure 17—Figure 22 at Puerto Rico NDBC buoy stations. Commonly used error statistics for all these parameters are shown in Table 2—Table 5. Based on the error statistics, the simulation period with the highest skill for simulating water levels and wave parameters, at either Florida or Puerto Rico, is May 2012, though overall most model predictions have reasonably good skill particularly when considering the buoys closest to the proposed arrays. The water level results at Vaca Key (8723970) have low skill particularly for RMSE and R, which is likely because it is located near islets that would require higher model grid resolution in that region to be properly resolved hydrodynamically.

The model successfully predicted not only the tidal range but also the spring-neap tidal cycle. The model also captured the non-tidal variability along Florida coast, in January and May 2012 (Figure 11 and Figure 12). However, the model tended to under-predict the water level during winter, November 2012 (Figure 13). Model results of wave climate matched the observed data reasonably at all stations around Florida (Figure 14—Figure 16).

At the Puerto Rico buoy stations, the model predictions for both water level and peak period are generally in good agreement with the observed data (Figure 17—Figure 22). Water levels at stations around Puerto Rico are a lot smaller than those in Florida. However, the model under-predicted the significant wave height at station San Juan (41053), Ponce (42085) and Rincon (41115) (Figure 20—Figure 22).

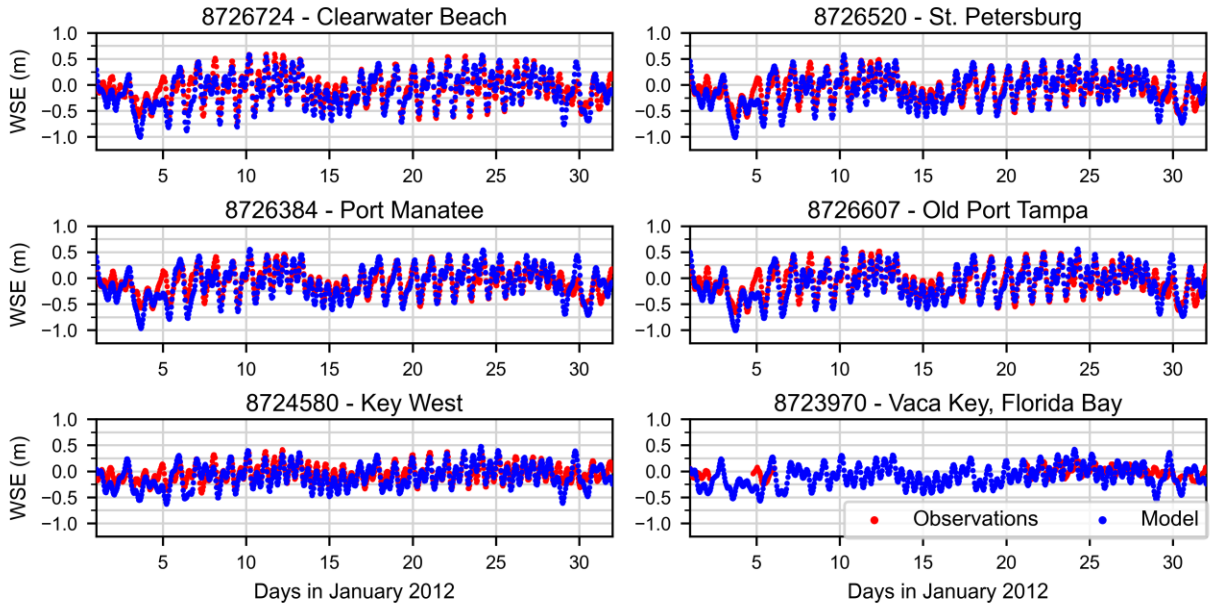

Figure 11. Water surface elevation at Florida stations for January 2012.

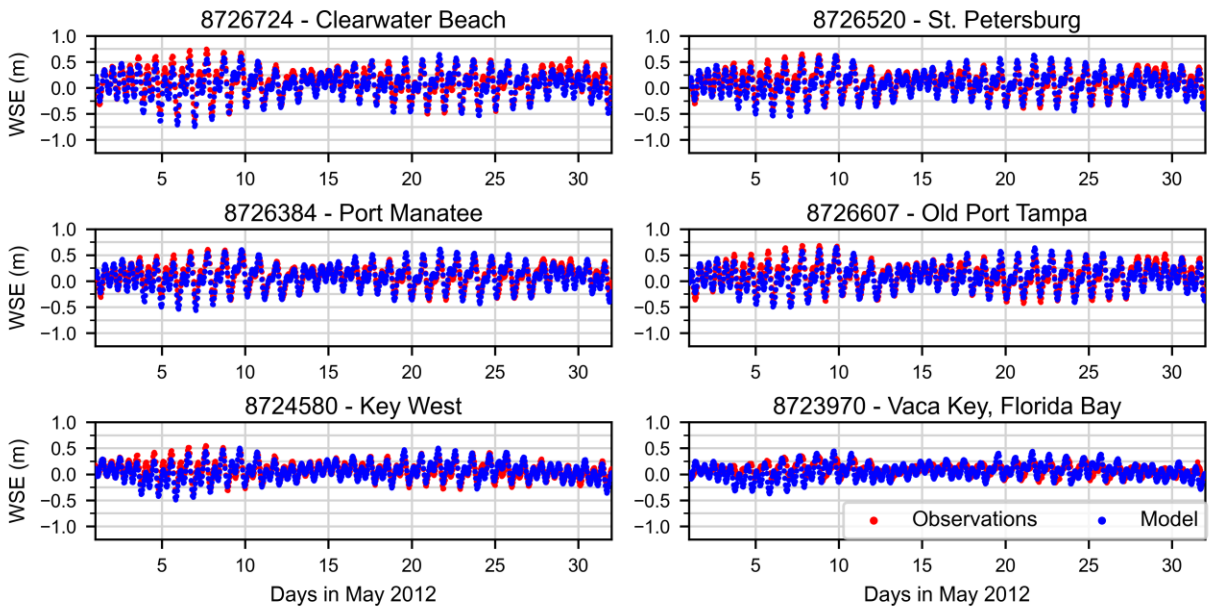

Figure 12. Water surface elevation at Florida stations for May 2012.

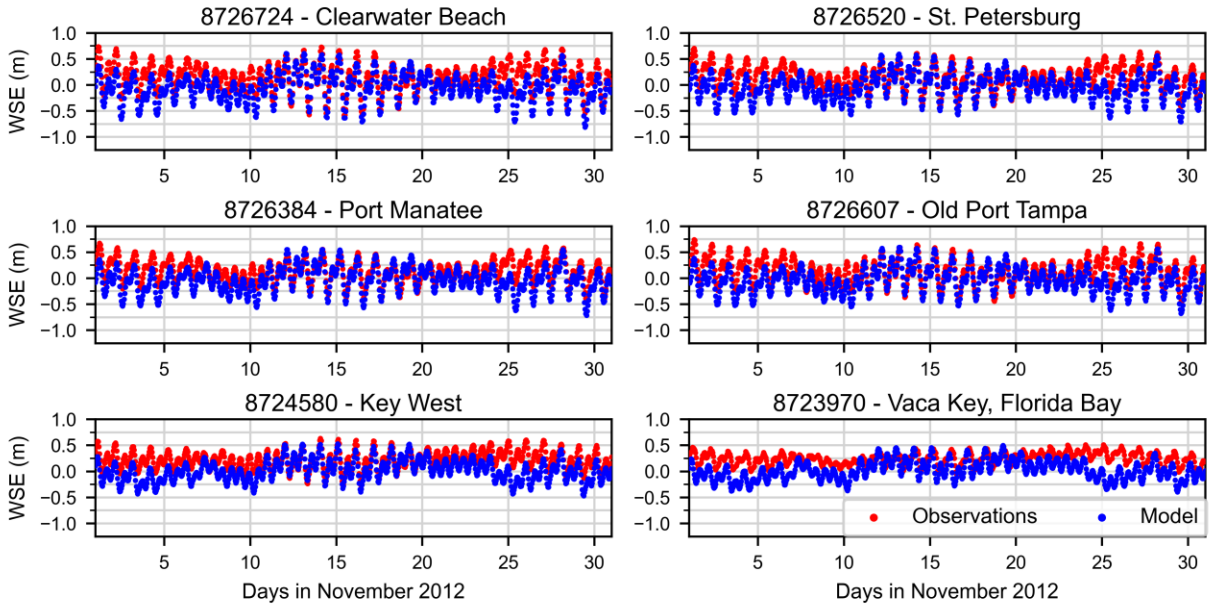

Figure 13. Water surface elevation at Florida stations for November 2012.

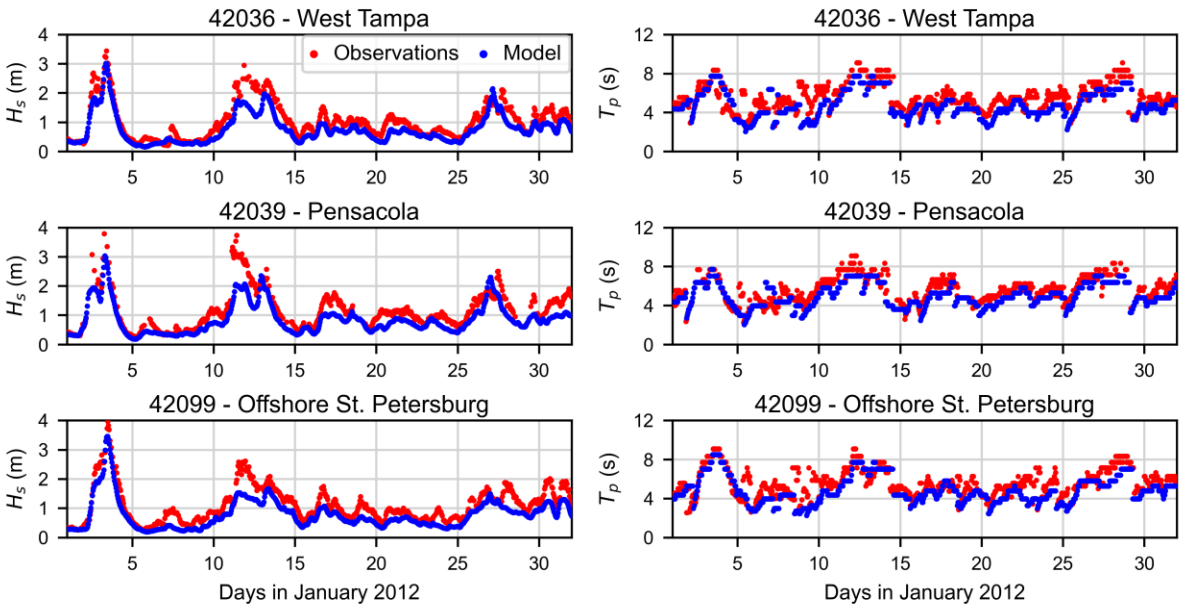

Figure 14. Significant wave height and peak period at Florida wave buoys for January 2012.

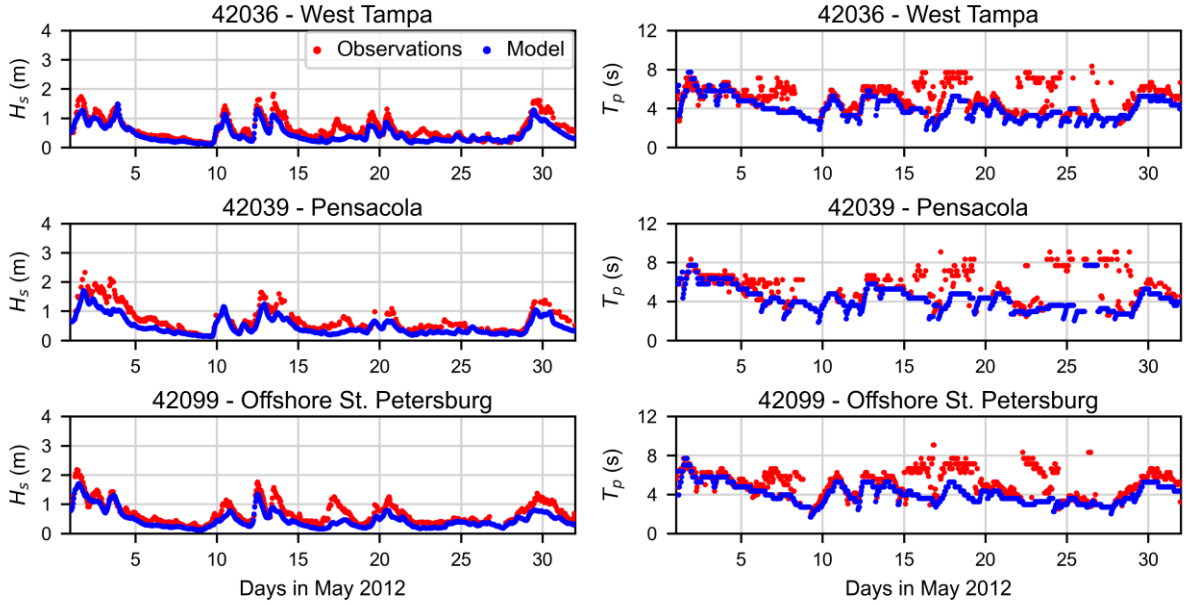

Figure 15. Significant wave height and peak period at Florida wave buoys for May 2012.

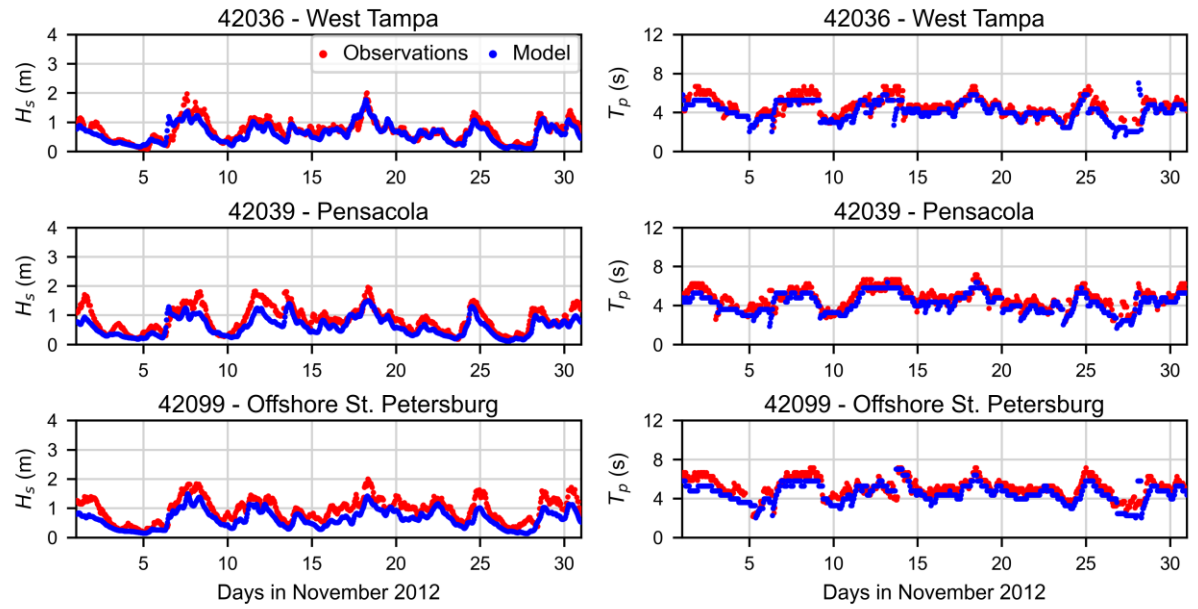

Figure 16. Significant wave height and peak period at Florida wave buoys for November 2012.

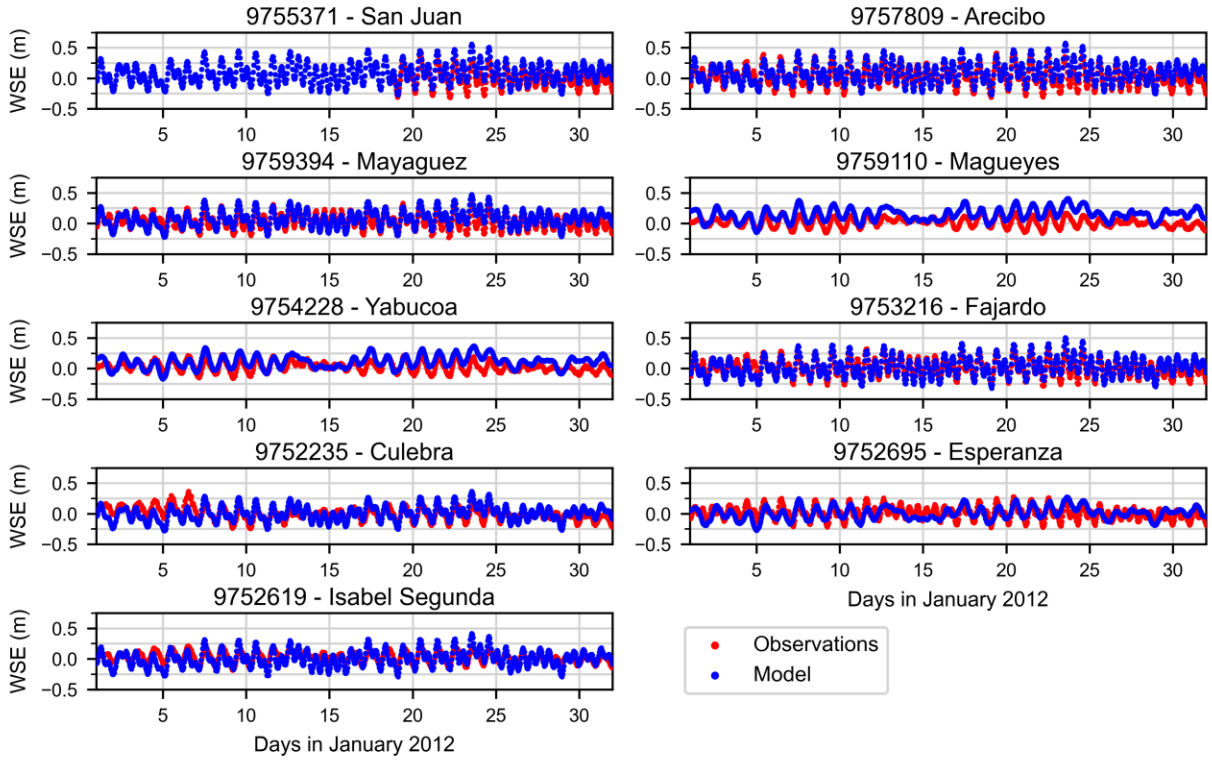

Figure 17. Water surface elevation at Puerto Rico stations for January 2012.

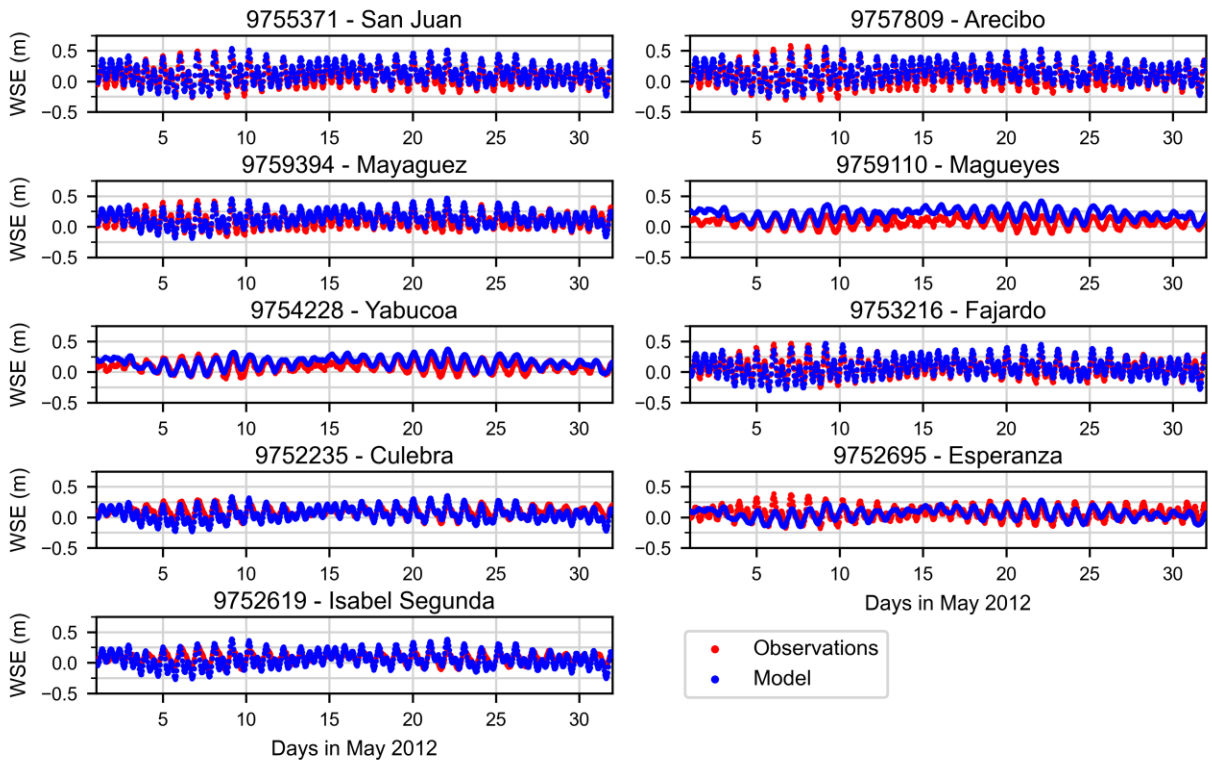

Figure 18. Water surface elevation at Puerto Rico stations for May 2012.

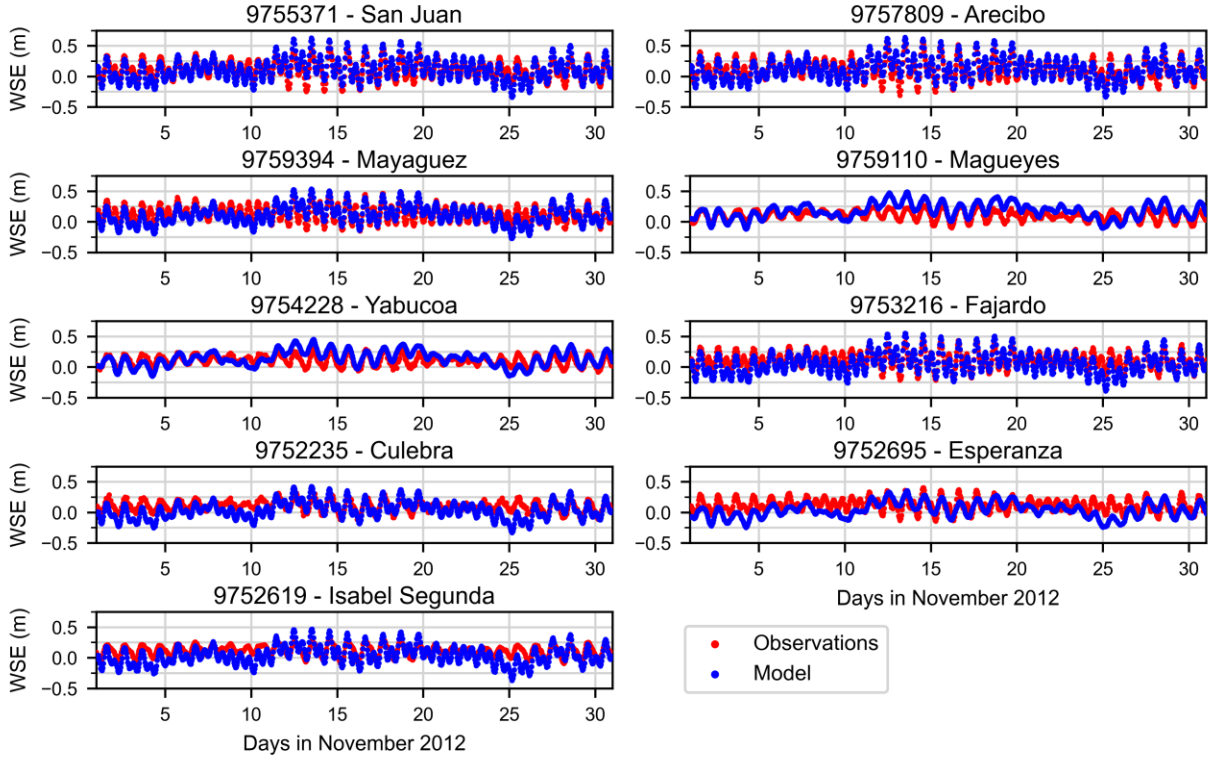

Figure 19. Water surface elevation at Puerto Rico stations for November 2012.

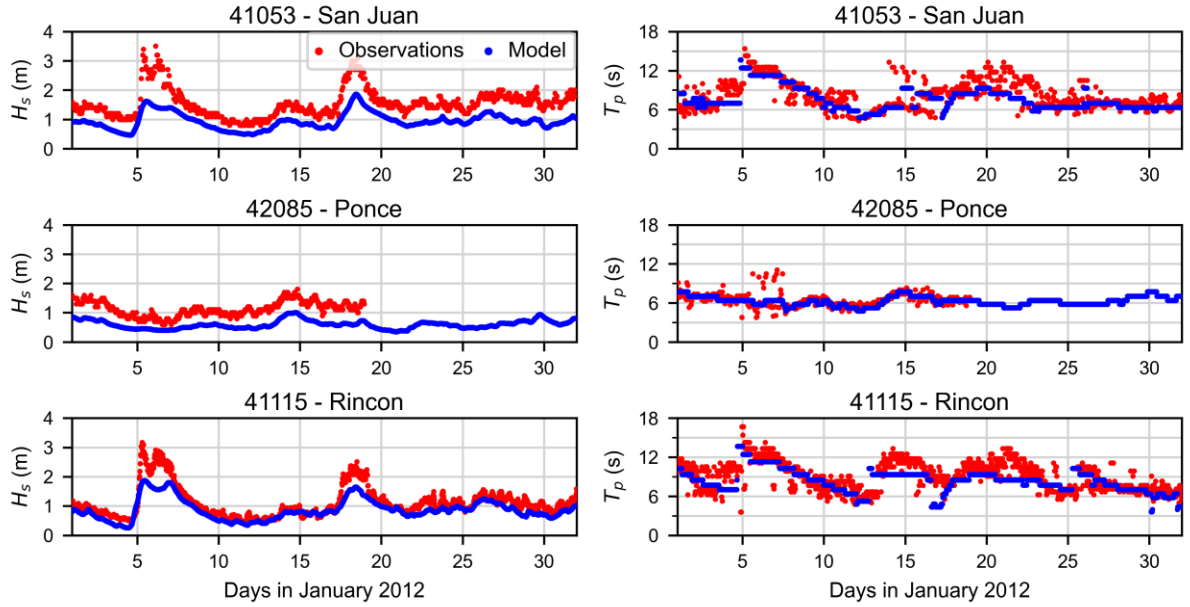

Figure 20. Significant wave height and peak period at Puerto Rico wave buoys for Jan. 2012.

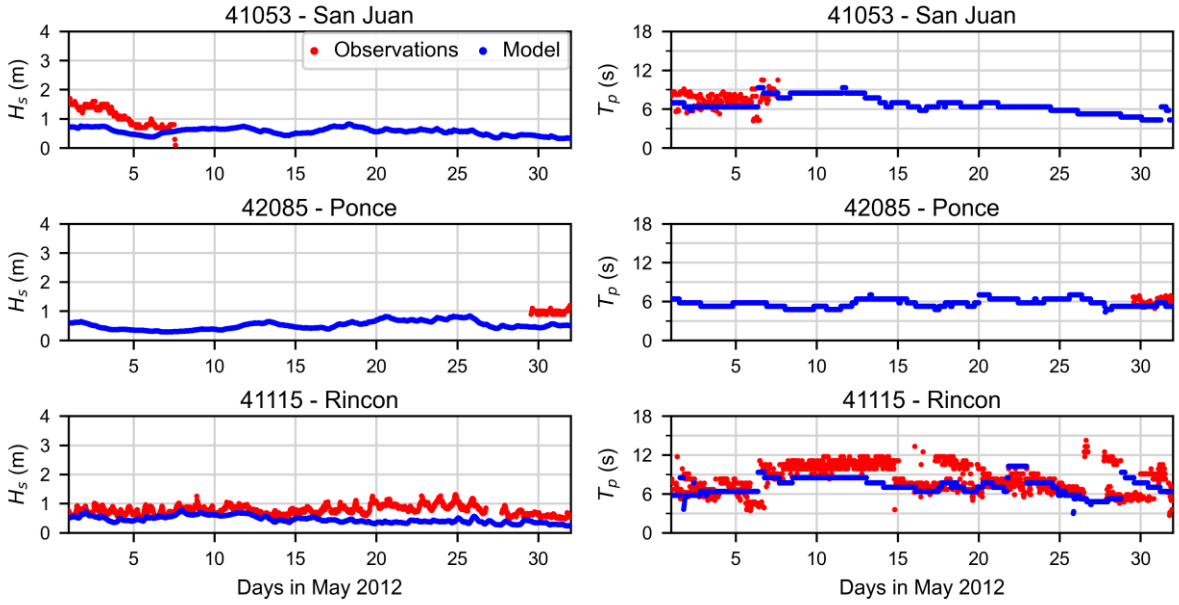

Figure 21. Significant wave height and peak period at Puerto Rico wave buoys for May 2012.

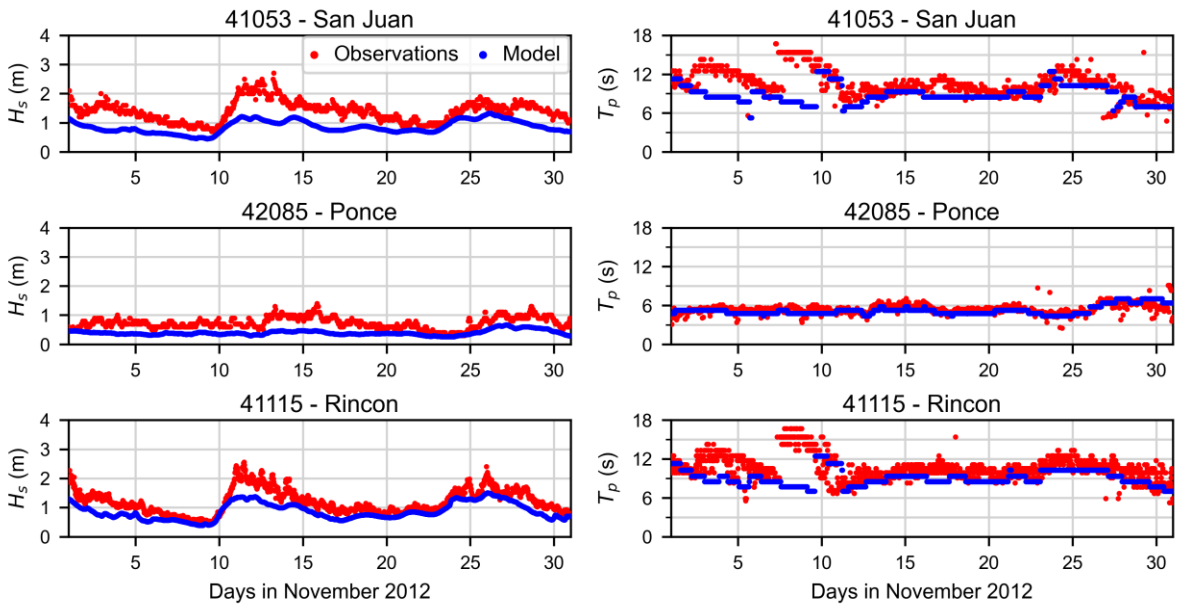

Figure 22. Significant wave height and peak period at Puerto Rico wave buoys for Nov. 2012.

Table 2. Error statistics for normal conditions in Florida at NDBC water level stations

	January 2012						May 2012						November 2012					
Station ID	N	RMSE	PE (%)	SI	bias	R	N	RMSE	PE (%)	SI	bias	R	N	RMSE	PE (%)	SI	bias	R
8726724	1489	0.18	4.04	-2.93	-0.05	0.85	1489	0.11	-27.7	0.89	-0.06	0.94	1441	0.25	3.99	1.69	-0.20	0.84
8726520	1489	0.17	-68.1	-2.81	-0.04	0.83	1489	0.12	6.74	0.97	-0.04	0.89	1441	0.24	-0.48	1.68	-0.18	0.78
8726384	1489	0.17	50.0	-2.33	-0.03	0.83	1489	0.11	-13.80	1.00	-0.03	0.89	1441	0.23	21.9	1.75	-0.17	0.77
8726607	1489	0.17	-3.19	-2.50	-0.03	0.84	1489	0.10	-12.30	0.90	-0.03	0.91	1441	0.23	12.7	1.79	-0.17	0.80
8724580	1489	0.15	22.9	-3.81	-0.05	0.75	1489	0.09	-4.36	1.17	-0.02	0.88	1441	0.26	-88.8	1.15	-0.21	0.71
8723970	646	0.22	-272	-11.05	-0.04	0.19	1489	0.17	-93.24	2.03	-0.03	0.18	1441	0.30	-111	1.21	-0.22	0.24

Table 3. Error statistics for normal conditions in Puerto Rico at NDBC water level stations

	January 2012						May 2012						November 2012					
Station ID	N	RMSE	PE (%)	SI	bias	R	N	RMSE	PE (%)	SI	bias	R	N	RMSE	PE (%)	SI	bias	R
9755371	630	0.14	46.4	-13.1	0.11	0.88	1489	0.09	-8.77	1.13	0.05	0.91	1441	0.11	12.7	0.99	0.00	0.81
9757809	1489	0.11	-23.7	4.50	0.07	0.84	1489	0.09	-4.14	1.15	0.06	0.91	1441	0.10	45.5	0.92	0.01	0.85
9759394	1489	0.09	-11.5	2.66	0.04	0.80	1489	0.07	35.7	0.68	0.03	0.88	1441	0.10	12.3	0.76	-0.02	0.77
9759110	1489	0.15	30.1	7.42	0.13	0.62	1489	0.14	76.1	1.87	0.13	0.73	1441	0.12	79.3	1.08	0.07	0.63
9754228	1489	0.11	32.6	3.45	0.08	0.61	1489	0.09	40.3	0.91	0.06	0.75	1441	0.10	1.66	0.95	0.03	0.60
9753216	1489	0.09	2.12	7.97	0.02	0.85	1489	0.07	13.9	1.01	0.01	0.90	1441	0.11	-8.44	1.05	-0.05	0.81
9752235	1489	0.12	-20.8	56.1	0.00	0.47	1489	0.09	-33.1	1.00	-0.04	0.66	1441	0.14	-57.9	1.31	-0.07	0.52
9752695	1489	0.11	-71.7	9.87	0.00	0.46	1489	0.10	-45.8	1.44	-0.01	0.52	1441	0.14	-73.1	1.20	-0.08	0.44
9752619	1489	0.11	-57.4	3.65	-0.03	0.61	1489	0.11	-27.0	1.35	-0.02	0.63	1441	0.14	-89.7	1.25	-0.08	0.61

Table 4. Error statistics for normal conditions in Florida at NDBC wave stations

		Hs						Tp					
	Station ID	N	RMSE	PE (%)	SI	bias	R	N	RMSE	PE (%)	SI	bias	R
Jan 2012	42036	706	0.34	-24.5	0.34	-0.26	0.94	697	1.22	-13.0	0.22	-0.77	0.73
	42039	604	0.42	-26.0	0.37	-0.31	0.92	603	1.01	-10.9	0.18	-0.67	0.81
	42099	699	0.38	-29.8	0.35	-0.32	0.95	699	1.21	-11.7	0.22	-0.72	0.74
May 2012	42036	705	0.22	-23.2	0.35	-0.16	0.92	622	1.62	-18.7	0.31	-1.09	0.48
	42039	408	0.31	-33.2	0.43	-0.25	0.96	383	2.11	-20.11	0.37	-1.34	0.35
	42099	680	0.26	-31.5	0.37	-0.21	0.92	667	1.67	-18.4	0.32	-1.11	0.43
Nov 2012	42036	708	0.19	-10.7	0.27	-0.10	0.88	640	0.75	-7.29	0.16	-0.39	0.73
	42039	711	0.30	-25.5	0.35	-0.23	0.90	683	0.75	-9.84	0.16	-0.50	0.83
	42099	711	0.35	-33.0	0.37	-0.31	0.93	701	0.81	-10.2	0.16	-0.55	0.81

Table 5. Error statistics for normal conditions in Puerto Rico at NDBC wave stations

		Hs						Tp					
	Station ID	N	RMSE	PE (%)	SI	bias	R	N	RMSE	PE (%)	SI	bias	R
Jan 2012	41053	737	0.65	-38.3	0.42	-0.60	0.90	737	1.75	-4.76	0.21	-0.63	0.67
	42085	407	0.54	-46.3	0.48	-0.52	0.90	406	0.86	-0.94	0.13	-0.14	0.58
	41115	1392	0.34	-19.6	0.30	-0.25	0.93	1392	1.95	-5.27	0.22	-0.75	0.60
May 2012	41053	159	0.55	-40.3	0.51	-0.49	0.86	159	1.49	-5.41	0.20	-0.61	0.21
	42085	60	0.49	-49.1	0.50	-0.49	0.04	56	0.79	-9.88	0.13	-0.63	0.29
	41115	1366	0.37	-39.0	0.47	-0.32	0.11	1366	2.32	-6.57	0.28	-0.97	0.26
Nov 2012	41053	719	0.59	-37.0	0.42	-0.53	0.72	719	2.83	-13.3	0.27	-1.69	0.18
	42085	706	0.37	-43.3	0.50	-0.33	0.68	704	0.74	-2.50	0.14	-0.19	0.50
	41115	1419	0.39	-25.6	0.32	-0.32	0.88	1419	2.68	-12.42	0.25	-1.57	0.01

3.2 Model validation for hurricane modeling

Hurricanes Irma and Maria were simulated using the ADCIRC+SWAN coupled model in 3D mode to validate its application for synthetic extreme events. For this comparison, measured buoy data was retrieved from NDBC at the stations shown in Figure 5.b; Figure 23 and Figure 24 show the comparisons of observed and modeled water surface elevation, wave heights and wave periods corresponding to the simulation of Hurricane Irma, while Figure 25 and Figure 26 show similar time-series for the simulation of Hurricane Maria. Gaps in the measurements are likely due to instrument malfunction under the influence of hurricanes which can generate abrupt movements. Commonly used error statistics for these parameters are shown in Table 6 and Table 7. The error statistics for Hurricane Maria show slightly higher model skill than for Hurricane Irma, though overall most model predictions have reasonably good skill. Unfortunately, there are some data gaps in the measured time series at the gauges closest to the proposed array (42085-Magueyes for water levels and 9759110-Ponce for waves) which introduce some uncertainty into the analysis. Generally, the prediction of significant wave height has higher skill than that of peak wave period.

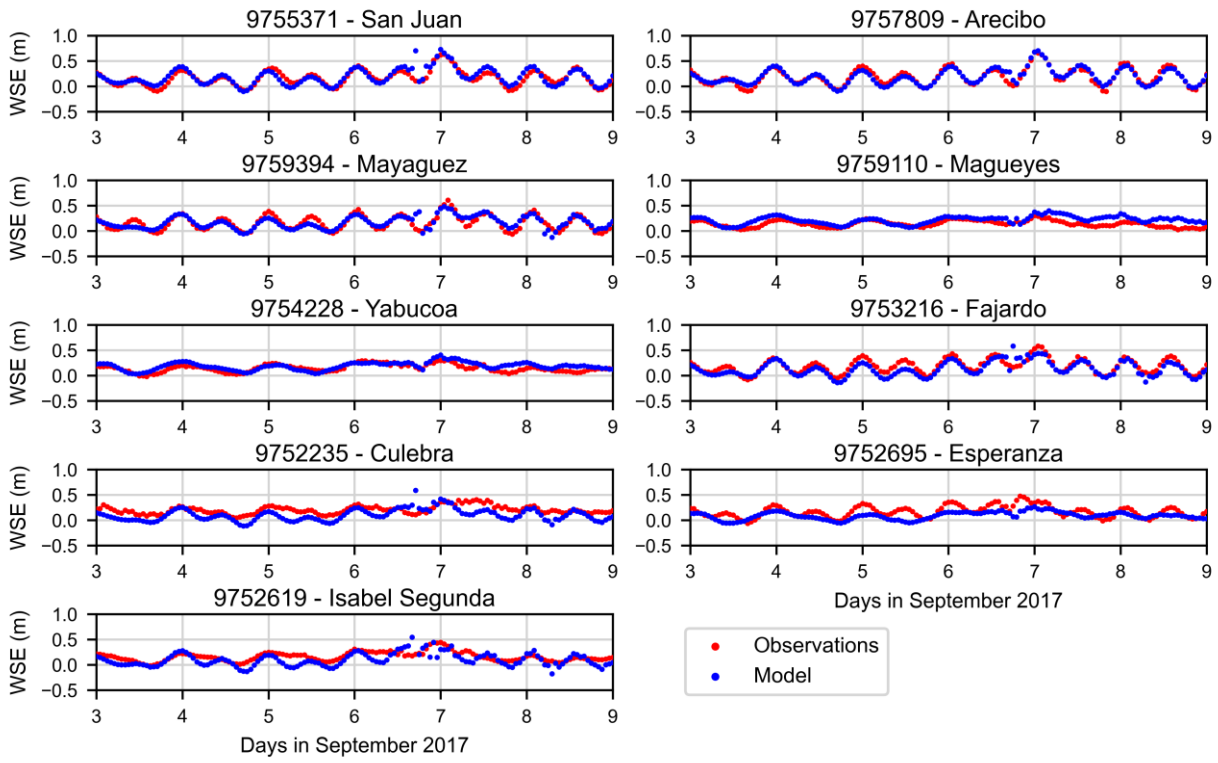

Figure 23. Water surface elevation at Puerto Rico stations for Hurricane Irma, September 2017.

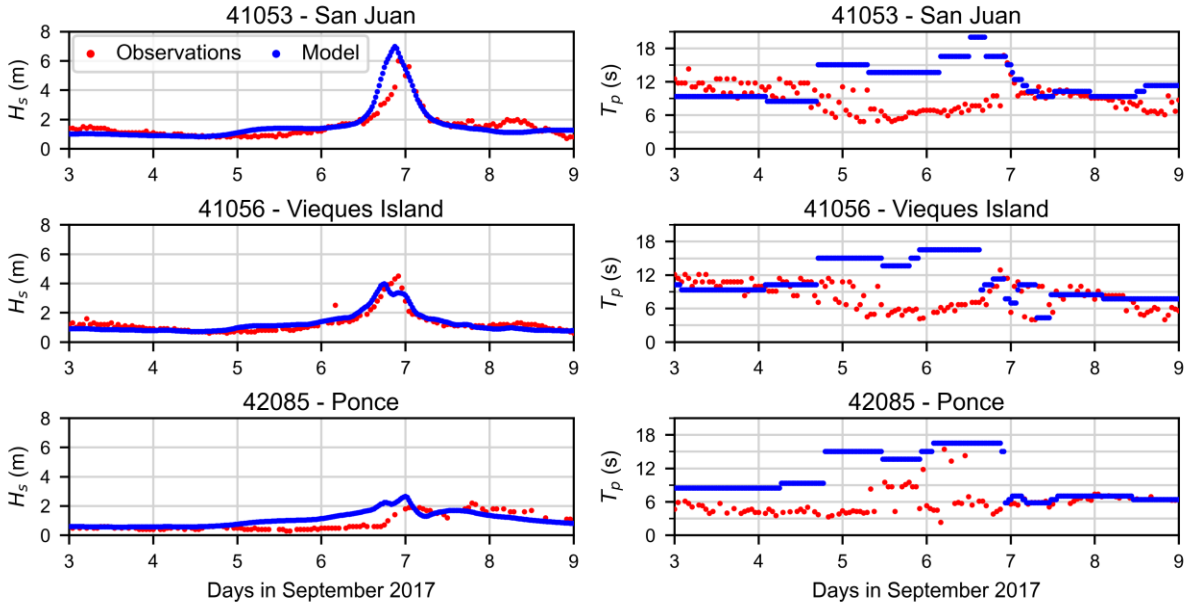

Figure 24. Significant wave height and peak period at Puerto Rico wave buoys for Hurricane Irma, September 2017.

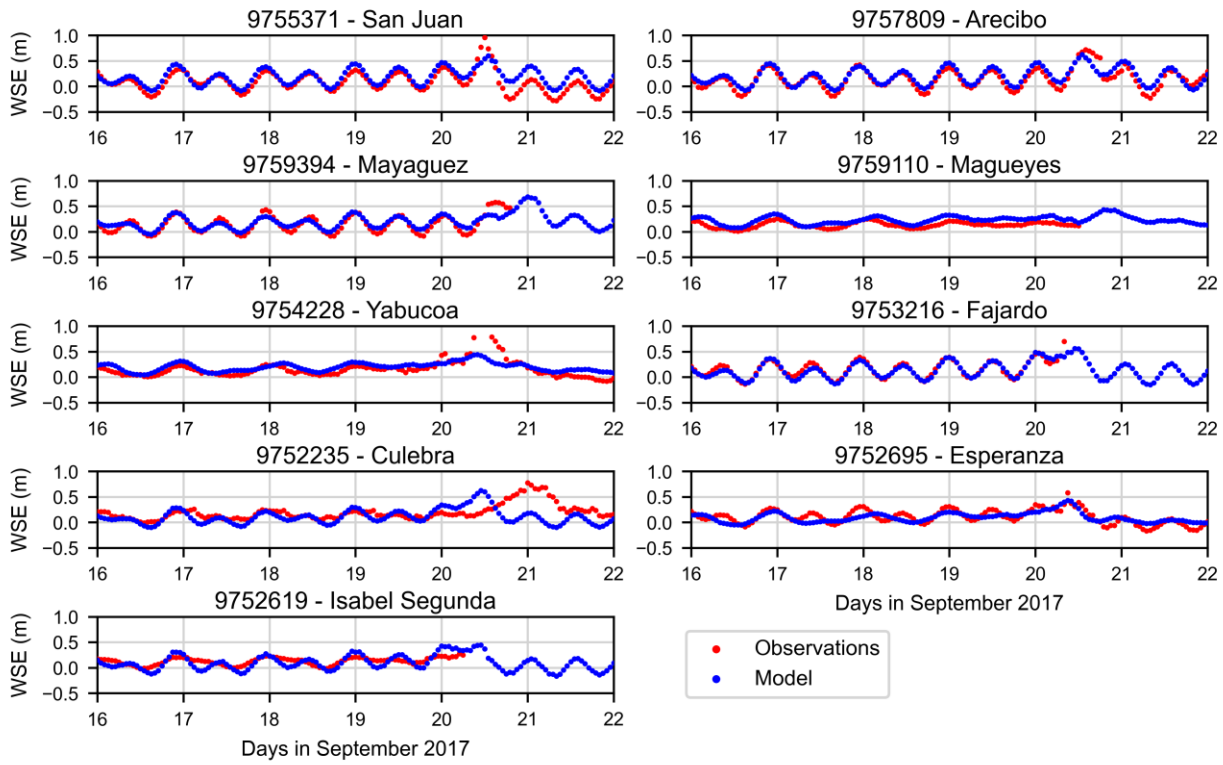

Figure 25. Water surface elevation at Puerto Rico stations for Hurricane Maria, September 2017.

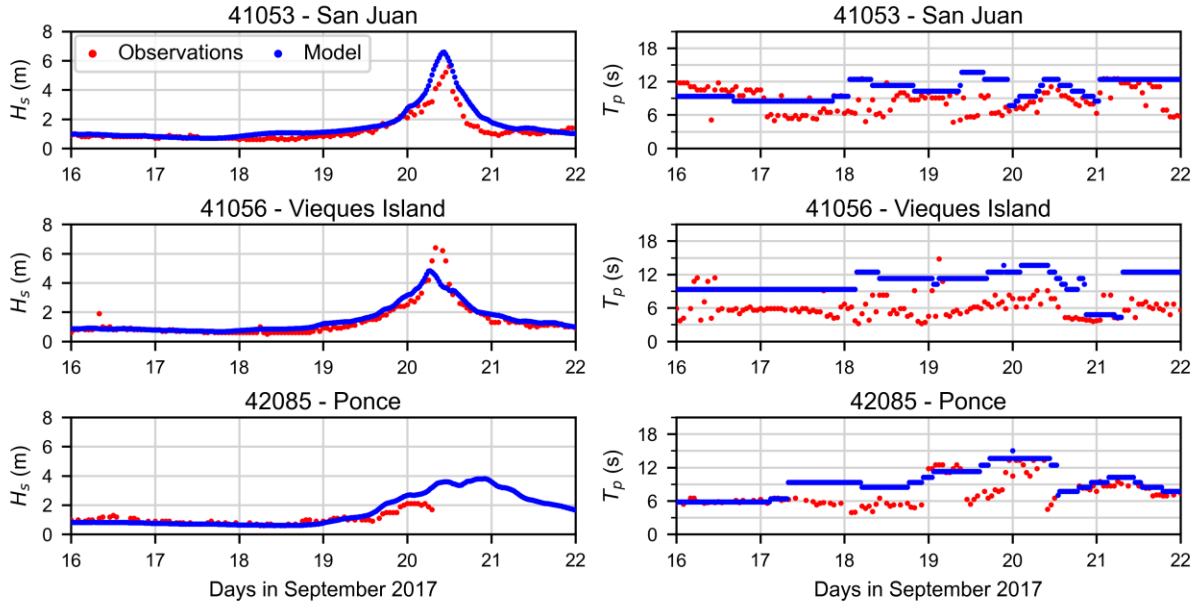

Figure 26. Significant wave height and peak period at Puerto Rico wave buoys for Hurricane Maria, September 2017.

Table 6. Error statistics for hurricane simulations in Puerto Rico at NDBC water level stations

	Irma						Maria					
Station ID	N	RMSE	PE (%)	SI	bias	R	N	RMSE	PE (%)	SI	bias	R
9755371	145	0.09	15.5	0.53	0.02	0.86	145	0.14	17.0	1.50	0.09	0.85
9757809	145	0.06	70.9	0.31	0.00	0.94	145	0.10	-50.0	0.69	0.05	0.90
9759394	145	0.08	64.6	0.52	0.00	0.80	116	0.09	-33.5	0.58	0.02	0.88
9759110	145	0.10	78.6	0.67	0.07	0.64	109	0.10	87.2	0.71	0.09	0.81
9754228	145	0.07	36.2	0.47	0.04	0.72	145	0.19	117	1.06	0.02	0.72
9753216	145	0.09	-43.6	0.50	-0.06	0.86	105	0.06	-35.4	0.35	-0.02	0.95
9752235	145	0.14	-55.7	0.69	-0.10	0.55	145	0.22	-42.6	1.11	-0.08	0.08
9752695	145	0.12	14.8	0.71	-0.08	0.62	145	0.09	-51.6	0.84	-0.01	0.74
9752619	145	0.16	-47.5	0.96	-0.05	0.50	103	0.10	9.51	0.74	-0.02	0.75

Table 7. Error statistics for hurricane simulations in Puerto Rico at NDBC wave stations

		Hs						Tp					
	Station ID	N	RMSE	PE (%)	SI	bias	R	N	RMSE	PE (%)	SI	bias	R
Irma	41053	145	0.59	4.2	0.38	0.06	0.89	145	5.43	46.91	0.61	2.91	-0.47
	41056	136	0.32	1.5	0.25	-0.01	0.91	136	5.22	49.33	0.63	2.71	-0.27
	42085	102	0.56	62.5	0.67	0.27	0.57	103	6.60	108.99	1.14	5.06	0.13
Maria	41053	145	0.54	24.5	0.43	0.32	0.96	144	3.24	31.3	0.38	1.96	0.12
	41056	137	0.42	16.4	0.31	0.13	0.93	137	5.02	83.53	0.83	4.39	0.27
	42085	72	0.41	1.3	0.37	0.08	0.92	107	2.94	31.6	0.39	1.85	0.59

3.3 Model outputs

For every model simulation, water levels, 3D currents, and wave parameters, were outputted at key locations in Florida and Puerto Rico. The Florida output stations include: 2 stations at the midpoint of each farm array near Tampa; 58 stations over a rectangular grid in the Tampa region aligned perpendicular to the coast; and 33 additional stations at points if interest (i.e., interior of Tampa and Bahia Honda Key) and along the western Florida coast (Figure 27).

The Puerto Rico output stations include: 3 stations at the midpoint of each farm arrays (Romero, Cayo Enrique and Cayo Media Luna); an offshore station at 17.9 N, 67.0367 W (a possible farm location to be considered by MBL); 286 stations over a rectangular grid aligned about the mean direction of synthetic hurricane tracks in the La Parguera region; and 396 data points elsewhere around Puerto Rico along 250 m contours up to 2000 m in depth (Figure 28).

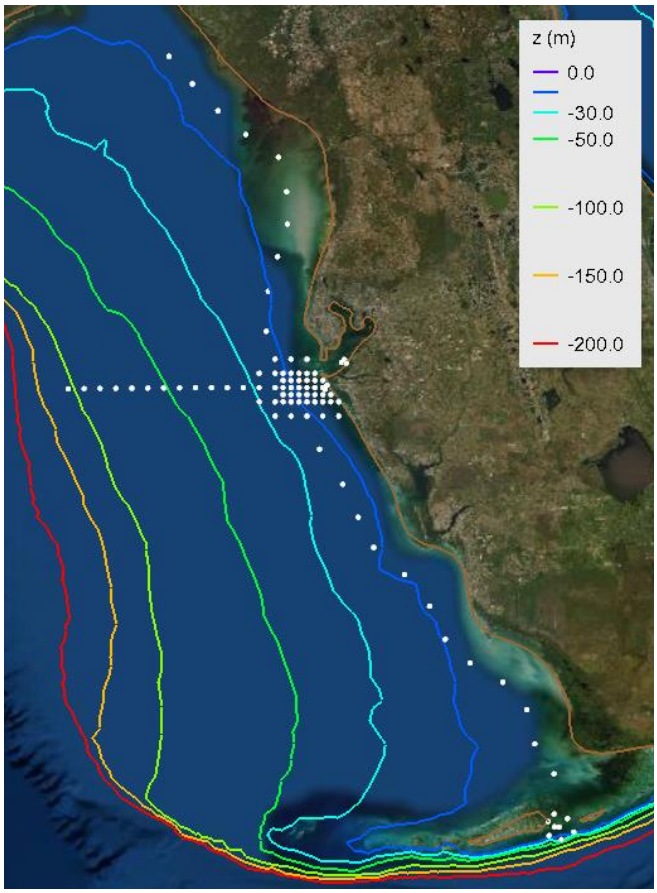

Figure 27. Florida output stations with counts shown for refence

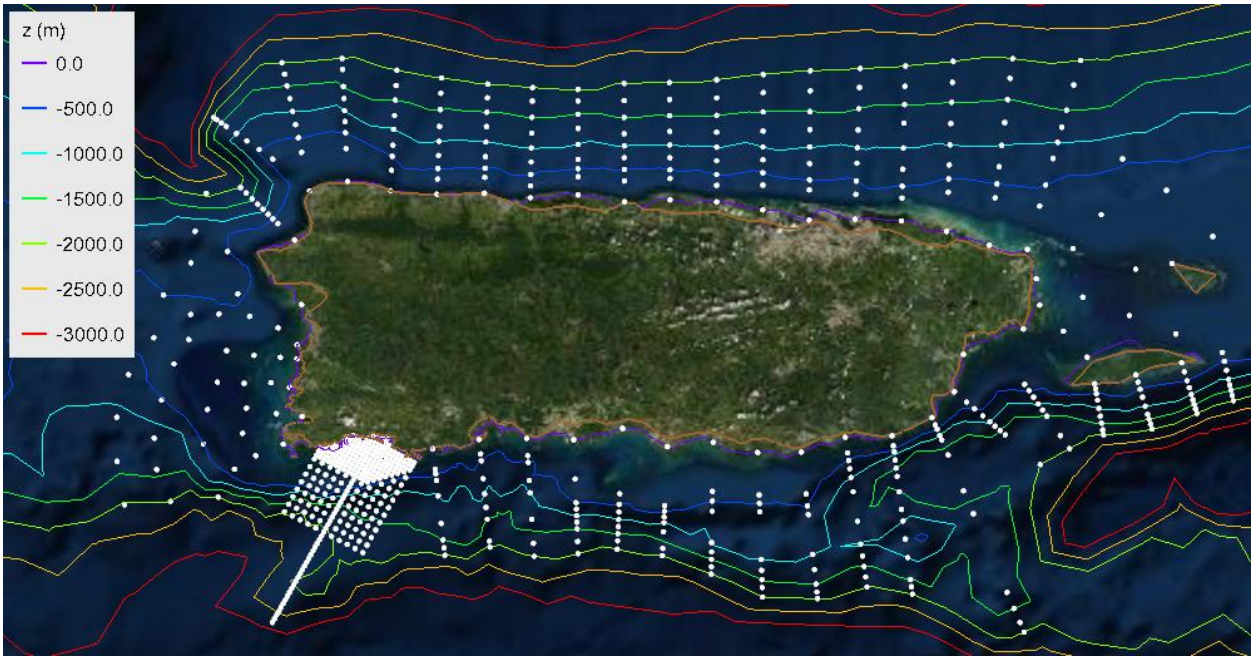

Figure 28. Puerto Rico output stations

3.4 Discussion

Figure 29 shows snapshots of modeled significant wave height and depth-averaged current magnitudes in the region of the cultivation sites in southwestern Puerto Rico at the time of greatest local intensity of Hurricane Maria. The model shows the sheltering effects of nearby reefs on waves and currents; the potential macroalgae array sites are exposed to diminished waves as compared to their surroundings but are also more exposed to local currents influenced by these features.

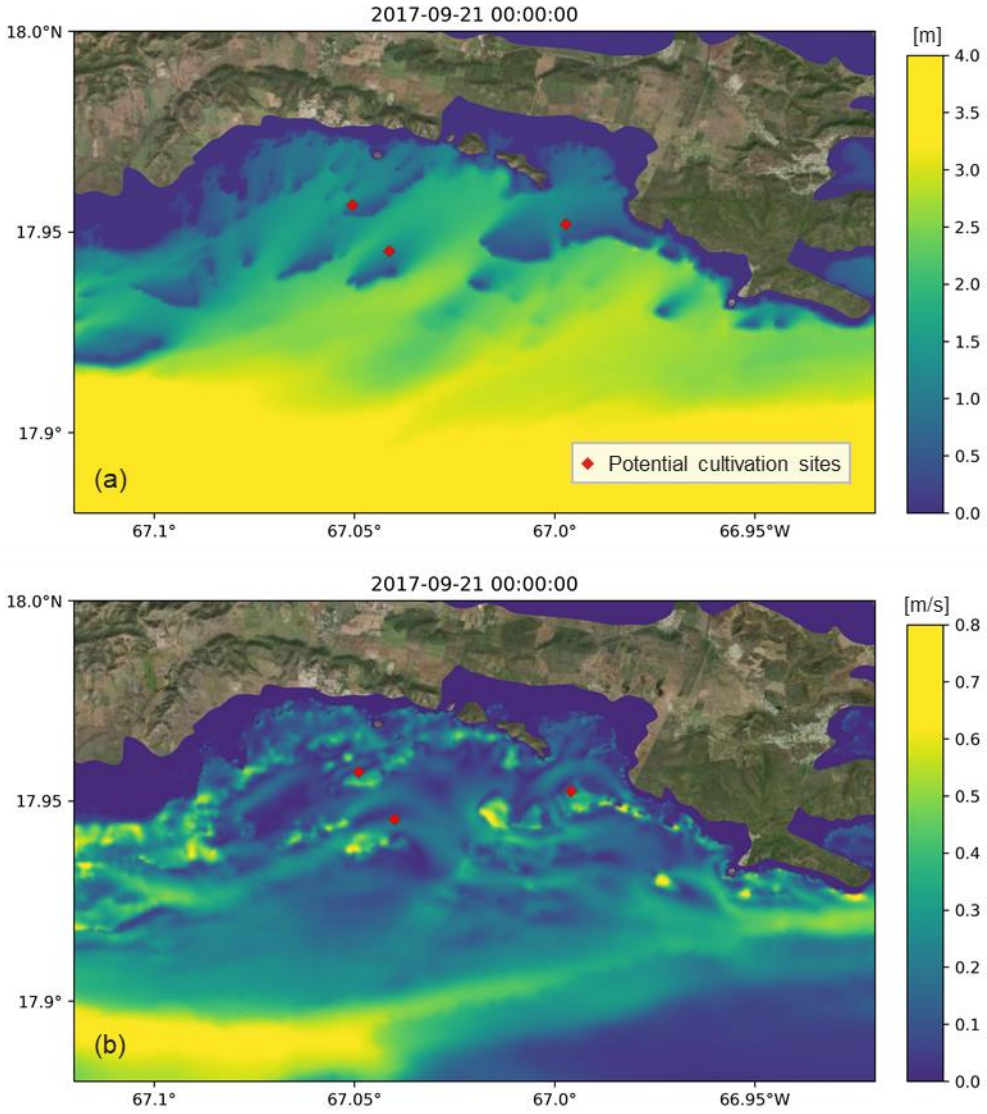

Figure 29. (a) Modeled significant wave height and (b) depth-average current magnitude in southwestern Puerto Rico under the influence of Hurricane Maria.

As an example of the influence of different hurricane severities, Figure 30, Figure 31 and Figure 32 show time series of key ocean and wave parameters for synthetic hurricanes of categories 1, 3 and 5, respectively, at the locations of the proposed cultivation arrays in Puerto Rico. As expected, these figures indicate that the arrays at Cayo Enrique and Arrecife Romero, being at

the most sheltered locations, will experience smaller waves than at Cayo Media Luna, however, the strongest induced currents are typically at the Arrecife Romero location.

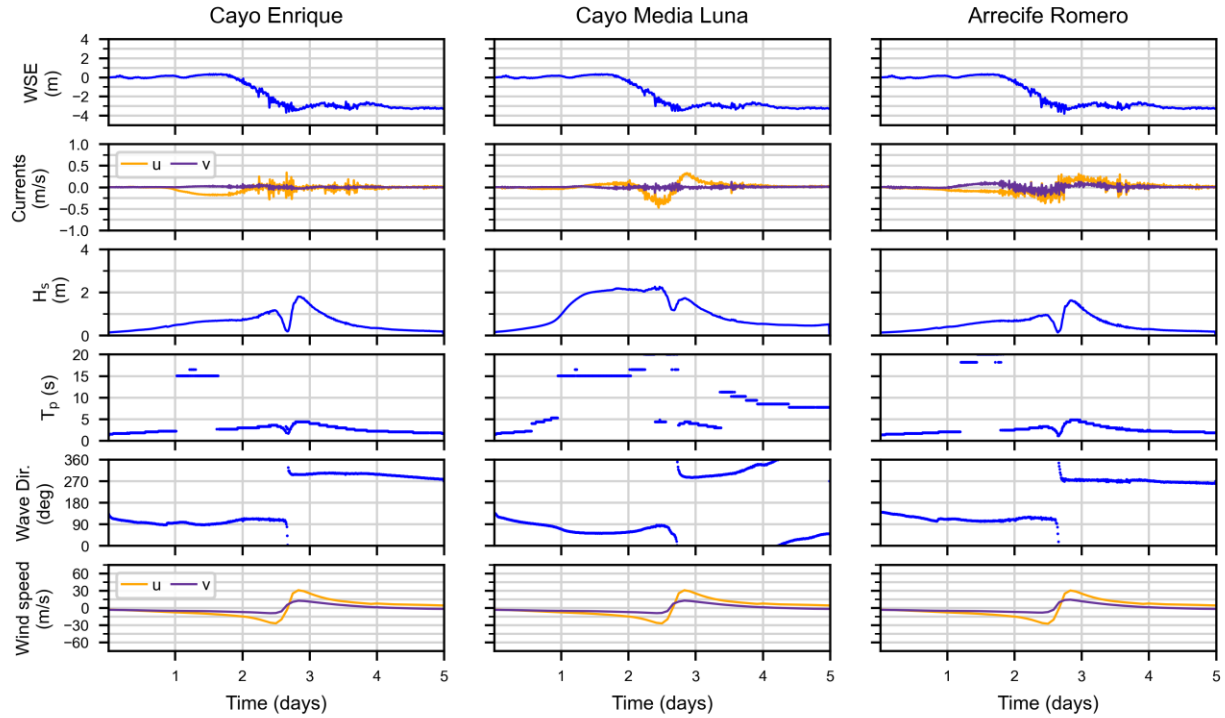

Figure 30. Sample time-series of output parameters of a Category 1 synthetic hurricane at Puerto Rico array sites.

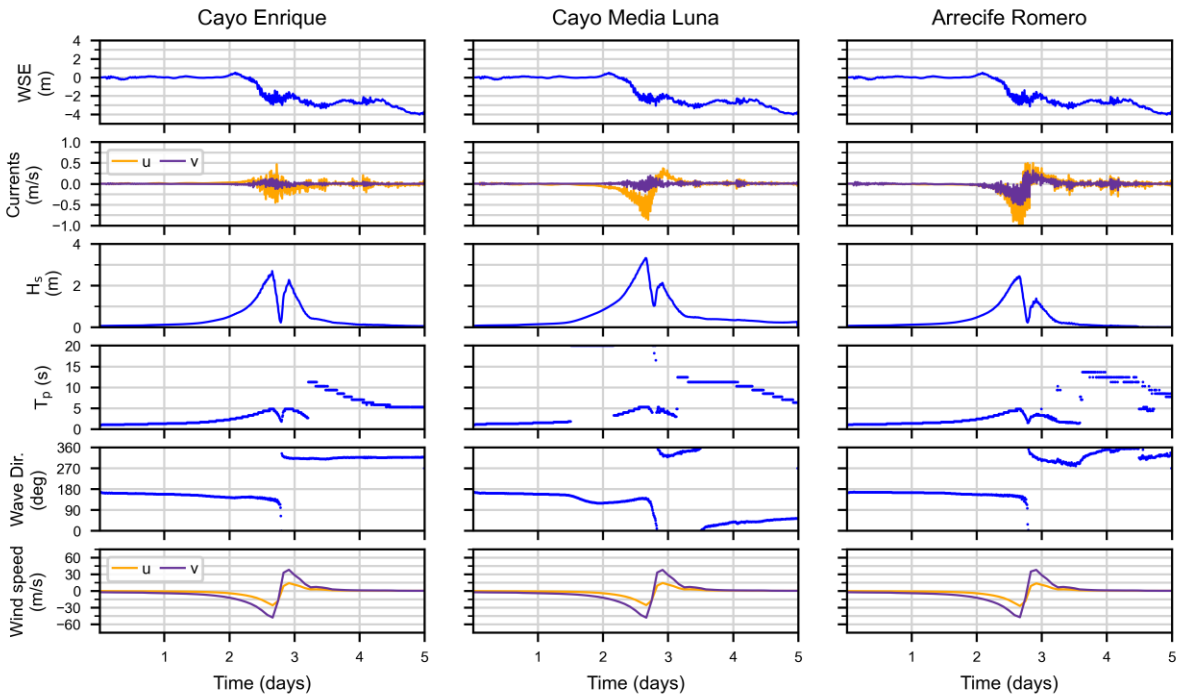

Figure 31. Sample time-series of output parameters of a Category 3 synthetic hurricane at Puerto Rico array sites.

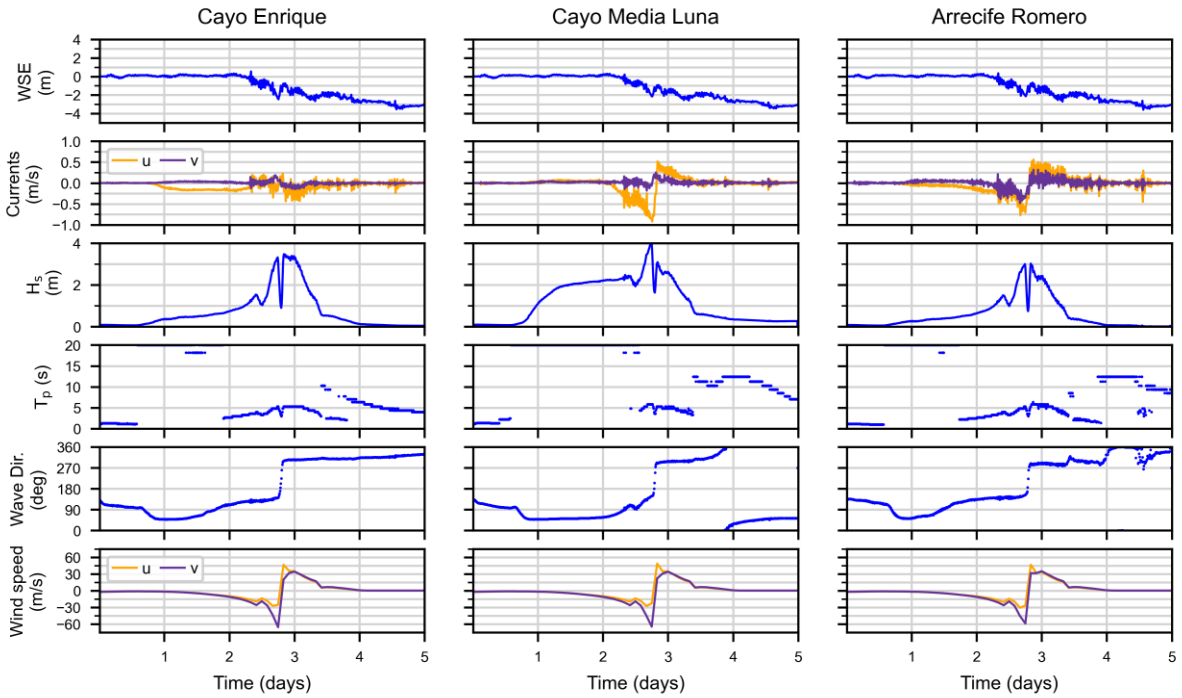

Figure 32. Sample time-series of output parameters of a Category 5 synthetic hurricane at Puerto Rico array sites.

For a more comprehensive analysis of the extreme conditions, we evaluate the maximum values of significant wave heights and currents for the ensemble dataset of synthetic hurricane simulations in comparison to the dataset of normal operation conditions. Figure 33 shows maximum values of significant wave height at the array sites for each simulation; hurricane events are plotted as circles colored by their category on the Saffir-Simpson scale and normal conditions runs are plotted as blue lines. The colored line drawn across the circles connects the average maximum values computed for each cluster of simulations. At all sites, the maximum significant wave height under normal conditions is below 1 m and increases to about 1.5 m and above for all hurricane simulations. A general trend is observed at all sites correlating an increase in hurricane intensities with an increase in maximum wave heights, noting that the trend is more confidently defined for lower category intensities since there are more representative events. Lower significant wave heights are observed at Arrecife Romero as compared to the other array location. Interestingly, events with longer sustained wind over time lead to greater significant wave heights even when the hurricane category is on the lower range.

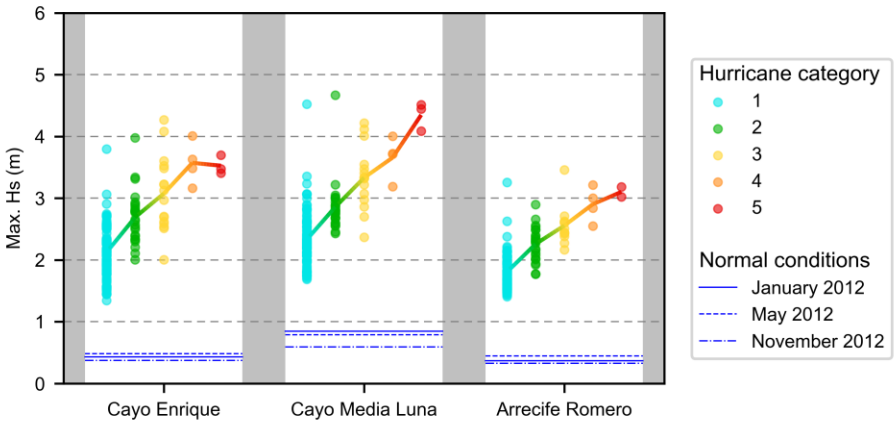

Figure 33. Maximum significant wave height for each hurricane simulation colored by storm intensity (colored circles, with category means connected by the colored line) and for each simulation of normal conditions (blue lines).

Figure 34 shows maximum values of current speed profiles at the three array sites for each synthetic hurricane and normal condition simulations. At all locations, the maximum current speeds are nearly zero throughout the water column under normal conditions and are noticeably greater for all synthetic hurricane events, particularly near the sea surface.

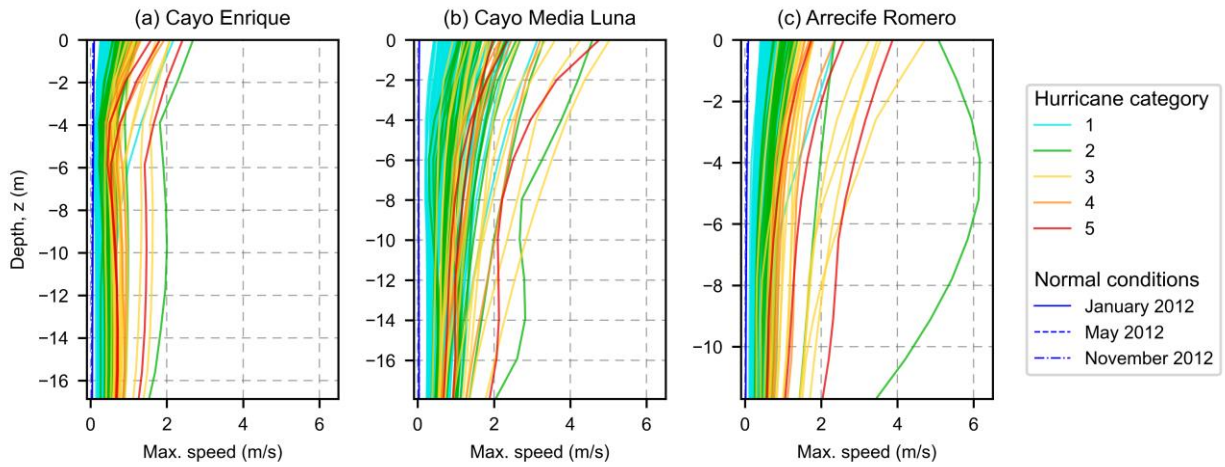

Figure 34. Profiles of maximum current speeds for each hurricane simulation colored by storm intensity (colored lines) and for each simulation of normal conditions (blue lines).

4.0 Summary and Recommendations

The PNNL team implemented a high-resolution coupled storm surge and wave model for support to MBL in the analysis and design of macroalgae cultivation farms in Florida and Puerto Rico.

The coupled ADCIRC+SWAN model, executed in 3D mode, was used to simulate normal operation and hurricane conditions, and was validated with available observed water level and wave data. Normal operation conditions were assessed based on three separate month-long simulations of the 2012 climatology, periods which were shown to be a good representation of long-term atmospheric conditions throughout a given year.

The probability distribution of velocity, storm surge and wave height under hurricane conditions was generated for the Puerto Rico project sites based on large ensemble simulations of synthetic hurricane events of various severities (Categories 1—5). Wind and pressure field were generated based on a subsampled dataset of synthetic hurricane tracks impacting the macroalgae sites in Puerto Rico.

Analyzing the error statistics of the results showed that the model performs well in predicting water levels, significant wave height, and peak wave period, for both normal operation and hurricane conditions. The primary error sources are likely data gaps in the measurements and coarser mesh resolution at buoys located away from project sites.

Hydrodynamic load analyses are critical to assess the growth and survivability of macroalgae due to wave- and current-induced disturbances (Jones, Gardner, and Bell 2015; Utter and Denny 1996) and thus help optimize macroalgae array designs. Simulated water level, 3D velocity, and wave climate driven by the synthetic hurricanes can be used to calculate the hydrodynamic load through water column and assess the risk induced by the extreme storm events. A necessary next step in the design of macroalgae cultivation arrays is an in-depth hydrodynamic load analysis based on the synthetic hurricane ensemble simulations.

5.0 References

Dietrich, J. C., J. J. Westerink, A. B. Kennedy, J. M. Smith, R. E. Jensen, M. Zijlema, L. H. Holthuijsen, et al. 2011. “Hurricane Gustav (2008) Waves and Storm Surge: Hindcast, Synoptic Analysis, and Validation in Southern Louisiana.” *Monthly Weather Review* 139 (8): 2488–2522. https://doi.org/10.1175/2011MWR3611.1.

Dietrich, J. C., M. Zijlema, J. J. Westerink, L. H. Holthuijsen, C. Dawson, R. A. Luettich, R. E. Jensen, J. M. Smith, G. S. Stelling, and G. W. Stone. 2011. “Modeling Hurricane Waves and Storm Surge Using Integrally-Coupled, Scalable Computations.” *Coastal Engineering* 58 (1): 45–65. https://doi.org/10.1016/j.coastaleng.2010.08.001.

Emanuel, Kerry, Sai Ravela, Emmanuel Vivant, and Camille Risi. 2006. “A Statistical Deterministic Approach to Hurricane Risk Assessment.” *Bulletin of the American Meteorological Society* 87 (3): 299–314. https://doi.org/10.1175/BAMS-87-3-299.

Emanuel, Kerry, and Richard Rotunno. 2011. “Self-Stratification of Tropical Cyclone Outflow. Part I: Implications for Storm Structure.” *Journal of the Atmospheric Sciences* 68 (10): 2236–49. https://doi.org/10.1175/JAS-D-10-05024.1.

Holland, Greg. 2008. “A Revised Hurricane Pressure–Wind Model.” *Monthly Weather Review* 136 (9): 3432–45. https://doi.org/10.1175/2008MWR2395.1.

Holzenthal, Elizabeth R., David F. Hill, and Meagan E. Wengrove. 2022. “Multi-Scale Influence of Flexible Submerged Aquatic Vegetation (SAV) on Estuarine Hydrodynamics.” *Journal of Marine Science and Engineering* 10 (4): 554. https://doi.org/10.3390/jmse10040554.

Jones, Timothy, Jonathan P. A. Gardner, and James J. Bell. 2015. “Modelling the Effect of Wave Forces on Subtidal Macroalgae: A Spatial Evaluation of Predicted Disturbance for Two Habitat-Forming Species.” *Ecological Modelling* 313 (October): 149–61. https://doi.org/10.1016/j.ecolmodel.2015.06.026.

Joyce, B. R., J. Gonzalez-Lopez, A. J. Van der Westhuysen, D. Yang, W. J. Pringle, J. J. Westerink, and A. T. Cox. 2019. “U.S. IOOS Coastal and Ocean Modeling Testbed: Hurricane-Induced Winds, Waves, and Surge for Deep Ocean, Reef-Fringed Islands in the Caribbean.” *Journal of Geophysical Research: Oceans* 124 (4): 2876–2907. https://doi.org/10.1029/2018JC014687.

Langlois, Juliette, Jean-François Sassi, Gwenaelle Jard, Jean-Philippe Steyer, Jean-Philippe Delgenes, and Arnaud Hélias. 2012. “Life Cycle Assessment of Biomethane from Offshore-Cultivated Seaweed.” *Biofuels, Bioproducts and Biorefining* 6 (4): 387–404. https://doi.org/10.1002/bbb.1330.

Menetrez, Marc Y. 2012. “An Overview of Algae Biofuel Production and Potential Environmental Impact.” *Environmental Science & Technology* 46 (13): 7073–85. https://doi.org/10.1021/es300917r.

Milledge, John J., Benjamin Smith, Philip W. Dyer, and Patricia Harvey. 2014. “Macroalgae-Derived Biofuel: A Review of Methods of Energy Extraction from Seaweed Biomass.” *Energies* 7 (11): 7194–7222. https://doi.org/10.3390/en7117194.

Notoya, Masahiro. 2010. “Production of Biofuel by Macroalgae with Preservation of Marine Resources and Environment.” In *Seaweeds and Their Role in Globally Changing Environments*, edited by Joseph Seckbach, Rachel Einav, and Alvaro Israel, 217–28. Cellular Origin, Life in Extreme Habitats and Astrobiology. Dordrecht: Springer Netherlands. https://doi.org/10.1007/978-90-481-8569-6_13.

Rhodes, Christopher J. 2010. “Biofuel from Algae: Salvation from Peak Oil?” In *Seaweeds and Their Role in Globally Changing Environments*, edited by Joseph Seckbach, Rachel Einav, and Alvaro Israel, 229–48. Cellular Origin, Life in Extreme Habitats and

Astrobiology. Dordrecht: Springer Netherlands. https://doi.org/10.1007/978-90-481-8569-6_14.

Saha, Suranjana, Shrinivas Moorthi, Xingren Wu, Jiande Wang, Sudhir Nadiga, Patrick Tripp, David Behringer, Yu-Tai Hou, Hui-ya Chuang, Mark Iredell, Michael Ek, Jesse Meng, Rongqian Yang, Malaquias Mendez, Huug van den Dool, Qin Zhang, Wanqiu Wang, Mingyue Chen, Emily Becker, et al. 2011. "NCEP Climate Forecast System Version 2 (CFSv2) 6-Hourly Products." UCAR/NCAR - Research Data Archive. https://doi.org/10.5065/D61C1TXF.

———. 2011. "NCEP Climate Forecast System Version 2 (CFSv2) Selected Hourly Time-Series Products." UCAR/NCAR - Research Data Archive. https://doi.org/10.5065/D6N877VB.

Utter, B, and M Denny. 1996. "Wave-Induced Forces on the Giant Kelp Macrocystis Pyrifera (Agardh): Field Test of a Computational Model." *Journal of Experimental Biology* 199 (12): 2645–54. https://doi.org/10.1242/jeb.199.12.2645.